AD_____

Award Number: W81XWH-07-1-0656

TITLE: New Imaging Strategies for Prostate Cancer

PRINCIPAL INVESTIGATOR: Dr. Warren Heston

CONTRACTING ORGANIZATION: Cleveland Clinic Foundation
Cleveland, OH 44195

REPORT DATE: October 2010

TYPE OF REPORT: Final

PREPARED FOR: U.S. Army Medical Research and Materiel Command
Fort Detrick, Maryland 21702-5012

REPORT DOCUMENTATION PAGE

Form Approved
OMB No. 0704-0188

1. REPORT DATE *(DD-MM-YYYY)*	2. REPORT TYPE	3. DATES COVERED *(From - To)*
01-10-2010	Final	4 Sep 2007-3 Sep 2010

4. TITLE AND SUBTITLE

New Imaging Strategies for Prostate Cancer

5a. CONTRACT NUMBER

5b. GRANT NUMBER
W81XWH-07-1-0656

5c. PROGRAM ELEMENT NUMBER

6. AUTHOR(S)

Dr. Warren Heston

E-Mail: hestonw@ccf.org

5d. PROJECT NUMBER

5e. TASK NUMBER

5f. WORK UNIT NUMBER

7. PERFORMING ORGANIZATION NAME(S) AND ADDRESS(ES)

Cleveland Clinic Foundation
Cleveland, OH 44195

8. PERFORMING ORGANIZATION REPORT NUMBER

9. SPONSORING / MONITORING AGENCY NAME(S) AND ADDRESS(ES)

U.S. Army Medical Research and Materiel Command
Fort Detrick, Maryland 21702-5012

10. SPONSOR/MONITOR'S ACRONYM(S)

11. SPONSOR/MONITOR'S REPORT NUMBER(S)

12. DISTRIBUTION / AVAILABILITY STATEMENT

Approved for Public Release; Distribution Unlimited

13. SUPPLEMENTARY NOTES

14. ABSTRACT

Imaging prostate cancer could be desirable from the perspective of helping tell where the tumor is, which can also aid the choice of therapeutic approaches and as a means to quantitate the results of therapy. Best would be the availability of low molecular ligands that could be generated with positron containing radionucleotides given their high sensitivity. In this report we describe the development of these new ligands and their improved binding characteristics and our pursuit of structure activity modifications to identify the best ligands for developing as PET radioligands. We identified a number of 2,5 A nucleotide glutamate urea ligands with excellent binding activity for PSMA While these ligands had excellent activity in vitro, they did not demonstrate in vivo binding activity. However, based on their excellent activity we were able to generate other ligands based on the 2,5A structure that were active in vivo with excellent imaging characteristics. We also identified that while PSMA is a feature of the majority of prostate cancers, that those tumors expressing the TMPRSS/ERG fusion gene may have some attenuation in PSMA signal.

15. SUBJECT TERMS

Prostate Cancer, Prostate Specific Membrane Antigen, PSMA, Imaging

16. SECURITY CLASSIFICATION OF:			17. LIMITATION OF ABSTRACT	18. NUMBER OF PAGES	19a. NAME OF RESPONSIBLE PERSON
a. REPORT	b. ABSTRACT	c. THIS PAGE			USAMRMC
U	U	U	UU	50	19b. TELEPHONE NUMBER *(include area code)*

INTRODUCTION:

Our overarching aim is to develop new low molecular weight imaging agents for prostate cancer with the focus on the use of agents that can be detected by positron emitting tomography (PET) scanning. Our lab cloned the gene Prostate-Specific Membrane Antigen (PSMA) which encodes a protein that is expressed on normal prostate and further up-regulated in prostate cancer. We are interested not only in imaging but also in developing anti-tumor targeted therapeutic agents as well. It was during our studies on therapeutic targeting that we developed an agent tri-2',5'-oligoadenylate-C-(S)-2-[3-(R)-1-carboxy-2-methylsulfanyl-ethyl-ureido]-pentanedioic acid (2,5-A3-ZJ24) in collaboration with Hagen Cramer, a Ph.D. chemist employed by the Cleveland Clinic start-up company, Ridgeway Inc. Ridgeway designated the bi-functional compound **RB1033**. While the compound bound prostate cancer cells that expressed PSMA, it did not appear that the potential anti-growth effecter portion, the 2,5-A analogue was taken inside the cell. While disappointing in that regard, it demonstrated improved PSMA binding that it bound over 1000 fold more tightly to PSMA than the unmodified tri-2,5-A which exhibited no binding and 10 fold better than the unmodified targeting ligand Cys-CO-Glu. Thus it appeared that it could be developed as a novel imaging agent and these analogs are being pursued as novel low molecular weight analogs for imaging. Our initial plan was to modify this lead compound for imaging and to do structure-activity modifications to determine what modification would exhibit the best selectivity and affinity to pursue for radiolabeling with F-18 for imaging by PET.

BODY:

The statement of work for Task one is to perform structure-activity relationship studies of novel PSMA targeting ligands in months 1-18, and Task two follows with the performance of in vivo imaging and biodistribution studies in mice bearing the prostate tumor in months 19-36. We completed task one and the description of the synthetic work was provided in the prior progress report. A summary of compounds is listed in Table one.

We finished Task one and have started radiolabeled the compounds for imaging. Nude mice were implanted with PSMA positive LNCaP tumors. We were disappointed to observe no difference in initial uptake with in the first two hours of F18 labeled compound between tumors that expressed PSMA and those that didn't. We had been using the structure-activity data obtained from these studies to modify peptides and examine them for uptake in a system that utilizes photoluminescence. With those compounds we had observed that a peptide that was designed to take advantage of the results of the structural-activity relationships we observed in these studies did exhibit strong uptake when linked to an infra-red fluorescent reagent. So we then modified our 2,5-A nucleic acid compounds with the infra-red ligands and examined them for binding activity and found them to retain strong binding activity as well as described in for the next study. Table 1 summarizes the structure and biological activity of the conjugates which were fully described in the prior report for structure-activity studies. Following this is the synthetic comparison of infra-red ligand modification of a peptide mimic of the nucleotide derivatives and of the nucleotide derivatives, their binding activity, and their ability to be imaged using photoluminescence.

Table 1: Summary of biological activity of new compounds synthesized for Task one.

Compounds	IC_{50} (nM) (competitive binding)	IC_{50} (nM) (folate hydrolase)
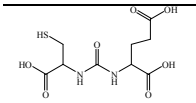 **1**	13.9	17.58
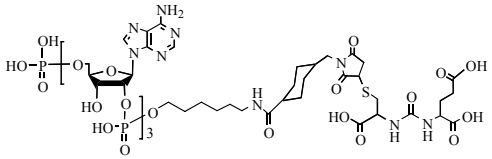 **7**	1.6	10.96
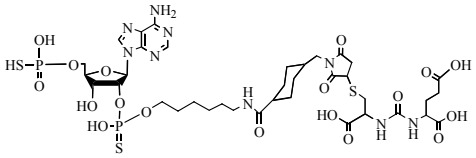 n=1, **11**	0.11	5.91
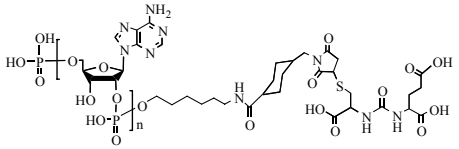 n=3, **12**	0.012	1.26

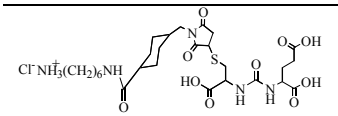 **16**	363.1	1750
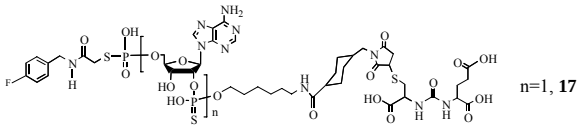 n=1, **17**	1.93	9.97
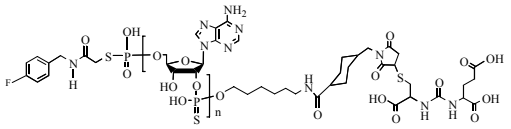 n=3, **18**	3.36	9.87
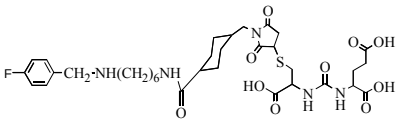 **19**	95.4	666.5
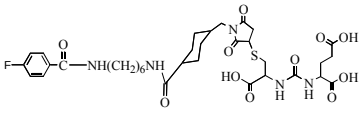 **20**	169.9	836.1

Summary for synthesis.

We reported the synthesis and biological activities of eight novel PSMA-based small compounds using the heterobifunctional linker succinimidyl 4-(N-maleimidomethyl)cyclohexane-1-carboxylate to conjugate amine-containing molecules and the parent compound (S)-2-(3-((S)-5-amino-1-carboxypentyl)ureido)pentanedioic acid (**1**). Previously, we have reported that inclusion of a C3-amine modified 2-5A trimer into **1** improved its binding affinity 10 times (*33*). Here we confirmed the observation by preparation of a series of compounds with or without 2-5A in their structures. It was observed that compounds with 2-5A in their structures showed significantly improved binding activity compared to those missing 2-5A. Extending the linker from C3 (**3**) to C6 (**12**) improved the binding activity more than 100 fold. It was also found that the binding affinity increased when the number of 2-5A increased from one (compound **11**) to three (compound **12**). Another interesting finding was that free 5'-phosphorothioate contributed to the activity greatly; replacement of 5'-phosphorothioate group (**12**) with phosphate group (**7**) or substitution of the free 5'-thioate group in **11** and **12** decreased their binding activity (**17** and **18**) dramatically.

The crystal structure of PSMA has been well elucidated The active site contains two zinc atoms, a smaller pharmacophore binding site (S1') and a larger nonpharmacophore pocket (S1). According to these elucidated crystal structure of PSMA, the glutamate portion (P1') of our compounds should be undoubtly located in the S1' pocket of PSMA, while the remainder of the molecule (P1) should be oriented in the S1 pocket. The S1 pocket contains a ~20 Å deep tunnel which narrows gradually. Extension of C3 (**3**) to C6 (**6**) might have optimized the steric hindrance, thus leading to better fit and binding characteristic. The S1 pocket has an adjacent hydrophobic pocket and it is arginine-rich. It has been reported that introduction of phenyl group can improved the binding activity. Similar to phenyl group, adenine group from 2-5A can form hydrophobic binding with the pocket. On the other side, the negatively charged phosphorothioate groups of 2-5A can form strong ion pairs with the positively charged guarnidine groups of arginine. These two factors working together offer the 2-5A containing compounds excellent affinity. Because the S1 pocket is positively charged, substitution of the free amine group in **16** neutralized its positive charge, hence gave improved binding activity as can be seen in compounds **19** and **20**. At this time, it's still not clear how the 5'-terminal phosphorothioate affect the binding. One hypothesis is that it might interact with the sulfhydryl group of cysteines in PSMA and form S-S bond, thus increase its binding affinity.

Summary for generation of Infra-red ligand and photoluminescence imaging.

Synthesis of peptides. Peptide synthesis was carried out by Fmoc chemistry. Peptide was synthesized starting with 0.1 mmol of Fmoc-glycine on Wang resin (Peptides International). Fmoc-deprotection at each cycle was carried out using 20% pipperidine in DMF. Coupling reactions were carried out using 3.3 equiv of Fmoc-amino acids in DMF activated with 3.3 equiv of HCTU and 5 equiv of diisopropylehtylamine (DIPEA) in DMF. Coupling of SMCC was achieved with 3.3 equiv of SMCC in DMF after the peptide sequence was built on the resin. Coupling of ZJ24 was performed by using 3.3 equiv of ZJ24 in DMF after coupling of SMCC to the peptide. The final peptide resin was washed with DMF and then dichloromethane and dried. Cleavage and deprotection were carried out using TFA/water/triisopropylsilane (950:25:25) for 1h, the resin was removed by filtration and washed with TFA. The combined filtrate was dried under nitrogen. The peptide was precipitated

by addition of diethyl ether and collected by centrifugation. The cleaved peptide was purified by preparative HPLC.

Conjugation to IRDye800. Conjugation of peptide to IRDye800 NHS ester (Li-Cor) was performed in anhydrous DMF. Basically, 100 nmol of peptide was dissolved in 100uL of DMF, to which 50nmol of IRDye800 in DMF was added. The reaction was carried out at room temperature for 3 hrs, then the mixture was injected into preparative HPLC for purification. Conjugation of 2-5A conjugate **12** to IRDye800 was achieved in the same condition except IRDye 800 maleimide (Li-Cor) was used instead of IRDye800 NHS ester.

High performance liquid chromatography (HPLC). HPLC was performed using a Shimadzu HPLC system equipped with a SPD-20V prominence UV/visible detector and monitored at a wavelength at 230nm or 778nm. The gradient used was 0-55% B over 45 minutes (A was 10 mM triethylammonium acetate TEAA, pH 7.0; B was acetonitrile). Preparative HPLC was achieved using SymmetryPrepTM C18 column (100mm × 19 mm × 5μm, Waters Corporation, Milford, MA, USA) at a flow rate of 3.0 ml/min. Analytical HPLC was performed using an analytical Symmetry C18 column (150 mm × 4.6 mm × 5μm, Waters Corporation, Milford, MA, USA) at a flow rate of 1 mL/min. Purities of all compounds were determined by analytical HPLC and were confirmed to be >95%.

Competitive Binding Assay. Briefly, LNCaP cells (5×10^5) were incubated with different concentrations of ligands in the presence of 12 nM N-[N-[(*S*)-1,3-dicarboxypropyl]carbamoyl]-*S*-[^{3}H]-methyl-L-cysteine in a total volume of 300 μL for 1 hour at 37^{o}C. The mixture was centrifuged at 1,000 g for 5 min at 4^{o}C, then washed three time with 500 μL of cold PBS. Finally, 4 mL of EcoLume^{TM} cocktail (MP Biomedicals) was added, and radioactivity was counted by scintillation counter. The concentration required to inhibit 50% of binding is determined (IC_{50}) by GraphPad Prism 3.0.

Table 2: Competitive binding activity of Dye800 conjugates

Compound	**IC50**

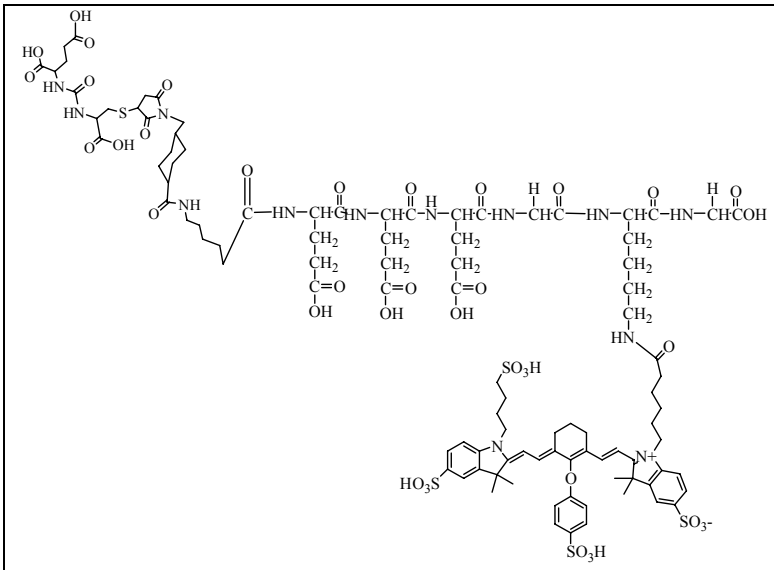 **ZS6-dE3-Dye800**	0.73nM
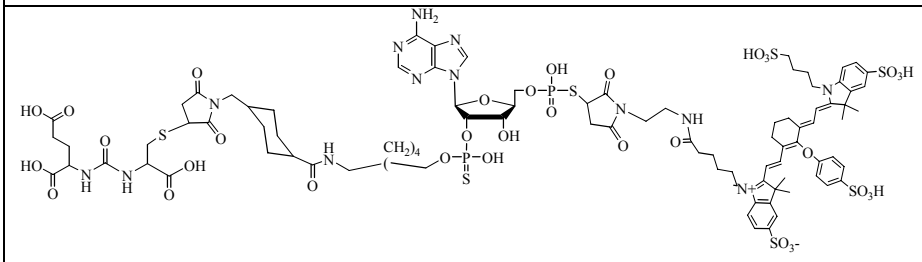 **2-5A-Dye800**	1.88nM

In vivo imaging studies. Six to eight weeks old SCID mice were implanted subcutaneously with 2×106 of PC3flu and PC3pip cells under the right and left arms respectively. Mice were imaged when tumors were at about 10mm in diameter. Imaging was performed on Maestro In Vivo Imaging system with each mouse received 1 nmol of IRDye800 conjugate in PBS through tale vein injection. Imaging was performed at different time points under near-infrared channel. During imaging, the temperature of imaging bed was adjusted to 37^{o}C. Mice received inhalation of isofluorane through a nose cone attached to the imaging bed. Twenty-four hours post injection, the mice were sacrificed by cervical dislocation and tissues such as liver, kidneys, tumors, heart, bladder and urinary gland were harvested for *ex vivo* imaging.

Summary of in vivo imaging studies.

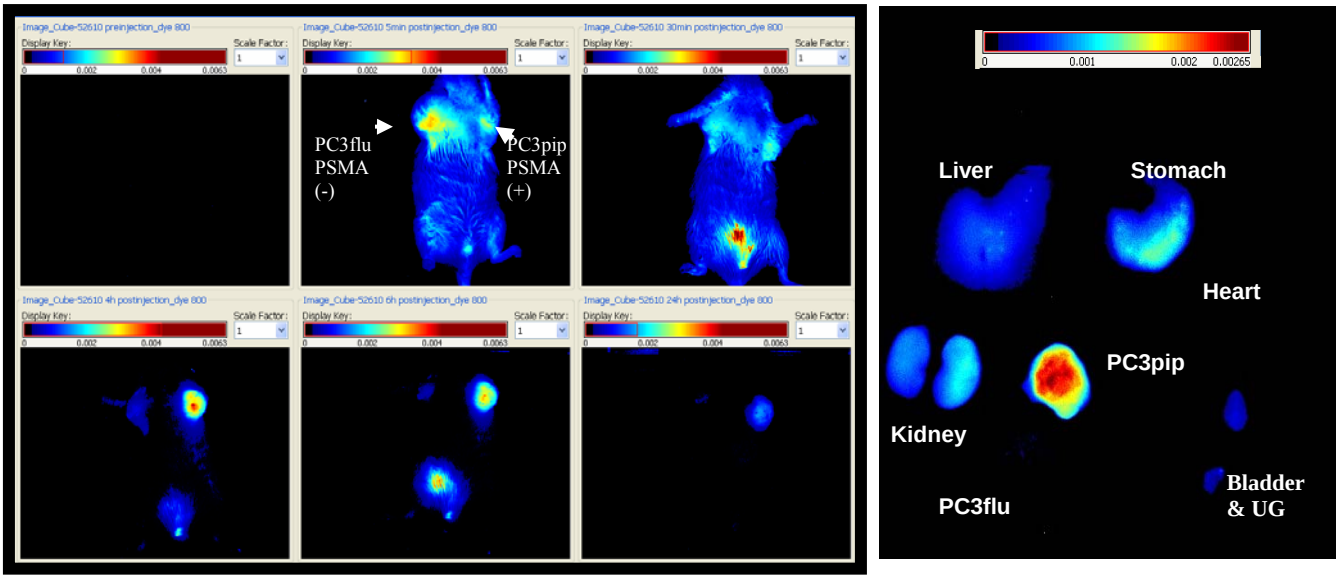

Figure 1: Left: In vivo imaging of ZS6-dE3-Dye800 conjugate using SCID mice through tale vein injection of 1 nmol of conjugate. Right: Imaging of organs 24 hours post injection.

As shown in Figure 1, conjugate ZS6-dE3-Dye800 showed selective tumor uptake in PSMA-positive PC3pip tumors, no uptake was observed in PSMA-negative PC3flu tumors. The results indicated the potential use of the conjugate for imaging studies.

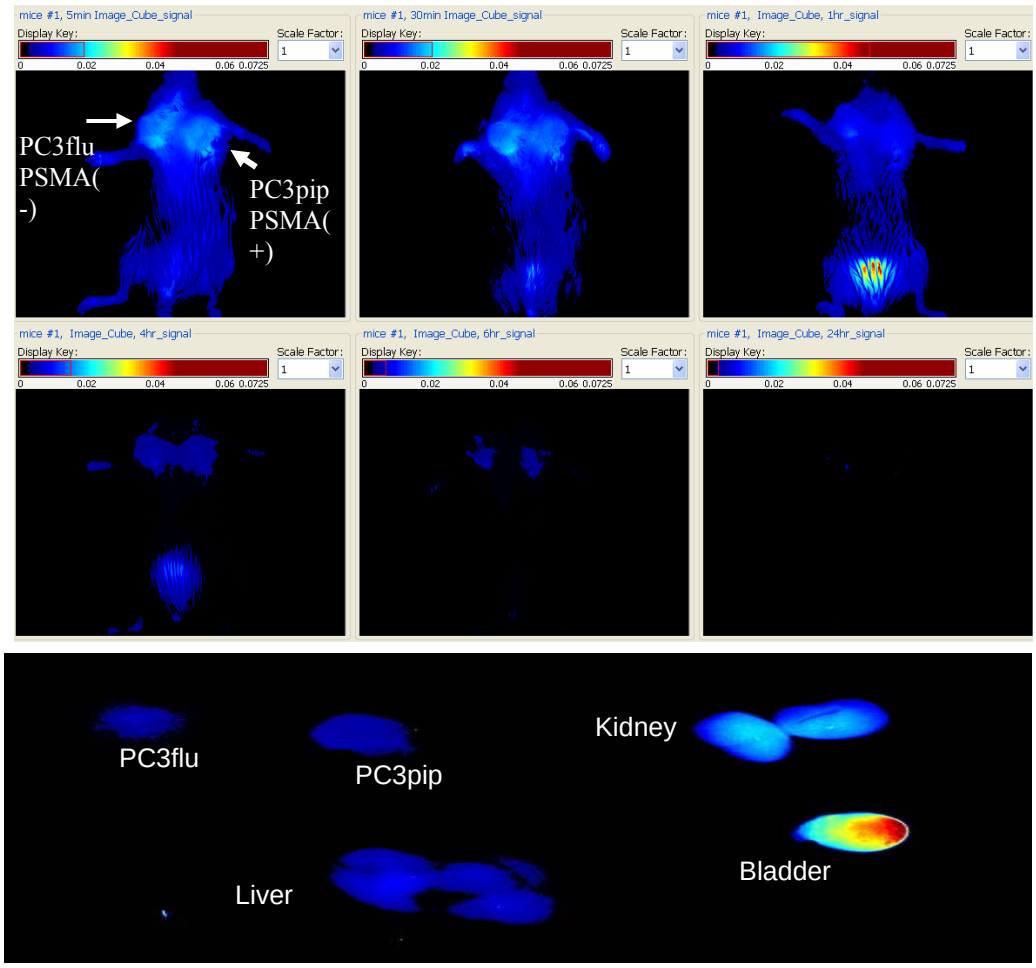

Figure 2: Upper: In vivo imaging of 2-5A-Dye800 conjugate using SCID mice through tale vein injection of 1 nmol of conjugate. Lower: Imaging of organs 24 hours post injection.

In contrast to the retention seen in Figure 1 for the anionic peptide that was designed to have anionic amino acids mimic the anionic positions of the nucleotide derivatives, the nucleotides derivatives themselves (Figure 2) demonstrated no retention.

Additional Study: Because of the finding that the most common genetic alteration in prostate cancer results in a fusion gene TMPRSS2/ERK and that occurs in 50% of patients and that PSMA is very very strongly expressed in 50% of patients we thought we should characterize the interaction of the two factors as that may help in understanding future imaging results as well as possibly explain the discrepant results in the imaging with the 2,5 A analogues. We found that the presence of the fusion gene that the androgen stimulation of the fusion gene causes a decrease in expression of PSMA. In patient samples our colleagues found a significant inverse correlation but the correlation was of a low. magnitude (Magi-Galuzzi M et al unpubli9shed).

Key Research Accomplishments:

1- We accomplished the synthesis of a number of 2,5A nucleotide derivatives.

2. We performed structure activity studies on those 2,5A nucleotide derivatives

3. We examined those 2,5A nucleotides for activity in preclinical imaging of prostate cancer tumors.

4. We examined the relationship between PSMA expression and the presence of TMPRSS2/Erg gene fusion.

Reportable Outcomes:

Publications:
Cramer H, Okicki JR, Rho T, Wang X, Silverman RH, Heston WD.: 2-5A ligands- a new concept for the treatment of prostate cancer. Nucleosides Nucleotides and Nucleic Acids, 26: 1471-1477, 2007.

Wang X, Yin L, Rao P, Stein R, Harsch KM, Lee Z, Heston WDW.: Targeted therapy of prostate cancer. J Cell. Biochem. 102: 571-579, 2007.

Wang X, Heston W, Tian H, Lee Z.: Fluorinated derivatives of N-asetylaspartylglutamate (NAAG) as substrates of prostate specific membrane antigen (PSMA). AACR 99th annual meeting April 12-16, 2008. Abst# 3180.

Xinning Wang; Warren Heston; Robert Silverman; Zhenghong Lee; Haibin Tian. Design of Small Molecules Targeting Prostate Specific Membrane Antigen. Innovative Minds in Prostate Cancer Today (IMPaCT), September 5-9, 2007, Atlanta, GA.

Wang X, Tian H, Lee Z, Heston WDW: Novel ligands targeting prostate specific membrane antigen (PSMA): synthesis and biologic evaluation. Innovative Minds in Prostate Cancer Today (IMPaCT), April 6-9th, Orlando FL PC060746-2365.

Yin L, Rao P, Elson P, Wang J, Itmann M, Heston WDW: Role of TMPRSS2/ERG gene fusion in negative regulation of PSMA expression . PLoS in press 2011.

Mentoring:
My Post-doctoral fellow Xinning Wang received a DoD Prostate Post-doctoral research fellowship award DAMD 7-00-1-0296; W81XWH-05-1-0600, titled Development of Chemotherapeutic agents targeting prostate-specific membrane antigen. This award helped us develop the current award in which she was a significant contributor to all of the chemical synthesis. She was promoted to a research associate in my lab and has since moved on to a faculty position at Case Western Reserve University Biomedical Dept section on Imaging.

I have also been mentoring a new faculty member in nuclear medicine, Dr. Steve Huang. Steve received a

Conclusion

We are at a loss to explain the difference between the peptide-IRDye800 conjugate and 2-5A-IRDye800. We hypothesize that it may be due to rapid metabolism of the nucleotides and plan to examine that further in the future. In terms of imaging we will move forward with the peptide derivatives which show excellent uptake and retention ratios. They are easy to synthesize and modify for imaging. Regardless, in spite of the excellent in vitro binding of the 2,5-A nucleotide derivatives, they appear to be poor agents for imaging in vivo.

PSMA expression and the presence of the TMPRSS2/ERG fusion gene are inversely correlated in the cell line VCaP , however work by our colleagues demonstrated they were also correlated inversely the clinical correlation was not a strong one (unpublished) so it is not likely that the presence of the fusion gene will diminish PSMA expression or its ability to be used as a target for imaging. .

References.

Cramer H, Okicki JR, Rho T, Wang X, Silverman RH, Heston WD.: 2-5A ligands- a new concept for the treatment of prostate cancer. Nucleosides Nucleotides and Nucleic Acids, 26: 1471-1477, 2007.

Wang X, Yin L, Rao P, Stein R, Harsch KM, Lee Z, Heston WDW.: Targeted therapy of prostate cancer. J Cell. Biochem. 102: 571-579, 2007.

Wang X, Heston W, Tian H, Lee Z.: Fluorinated derivatives of N-asetylaspartylglutamate (NAAG) as substrates of prostate specific membrane antigen (PSMA). AACR 99th annual meeting April 12-16, 2008. Abst# 3180.

Xinning Wang; Warren Heston; Robert Silverman; Zhenghong Lee; Haibin Tian. Design of Small Molecules Targeting Prostate Specific Membrane Antigen. Innovative Minds in Prostate Cancer Today (IMPaCT), September 5-9, 2007, Atlanta, GA.

Wang X, Tian H, Lee Z, Heston WDW: Novel ligands targeting prostate specific membrane antigen (PSMA): synthesis and biologic evaluation. Innovative Minds in Prostate Cancer Today (IMPaCT), April 6-9th, Orlando FL PC060746-2365.

Yin L, Rao P, Elson P, Wang J, Itmann M, Heston WDW: Role of TMPRSS2/ERG gene fusion in negative regulation of PSMA expression . PLoS in press 2011.

Also see submitted article in appendix

Wang X, Tian H, Lee Z, Heston WD: Synthesis and biological evaluation of new ligands for future imaging of prostate cancer by targeting prostate specific membrane antigen (PSMA). Submitted.

Role of TMPRSS2-ERG gene fusion in negative regulation of PSMA expression

Lihong Yin[1], Pravin Rao[2], Paul Elson[3], Jianghua Wang[4], Michael Ittmann[4], Warren D.W. Heston[1,2]

[1]Department of Cancer Biology, Cleveland Clinic

[2] Glickman Urological and Kidney Institute, Cleveland Clinic

[3] Department of Quantitative Health Sciences, Cleveland Clinic, Cleveland, Ohio

[4] Department of Pathology and Immunology, Baylor College of Medicine, and the Michael E. DeBakey VAMC, Houston, Texas

Requests for reprints: Warren D.W. Heston, Department of Cancer Biology ND50, Cleveland Clinic, Lerner Research Institute, 2111 East 96th street, Cleveland, OH 44106. Phone: 216-444-8181; Fax: 216-445-0610; E-mail: hestonw@ccf.org.

Abstract

Prostate specific membrane antigen (PSMA) is over-expressed in prostatic adenocarcinoma (CaP), and its expression is negatively regulated by androgen stimulation. However, it is still unclear which factors are involved in this down-regulation. *TMPRSS2-ERG* fusion is the most common known gene rearrangement in prostate carcinoma. Androgen stimulation can increase expression of the *TMPRSS2-ERG* fusion in fusion positive prostate cancer cells. The purpose of this investigation is to determine whether PSMA expression can be regulated by the *TMPRSS2-ERG* gene fusion. We employed two PSMA positive cell lines: VCaP cells, which harbor *TMPRSS2-ERG* fusion, and LNCaP cells, which lack the fusion. After 24 hours of androgen treatment, TMPRSS2-ERG mRNA level was increased in VCaP cells. PSMA mRNA level was dramatically decreased in VCaP cells while it only has moderate change in LNCaP cells. Treatment with the androgen antagonist flutamide partially restored PSMA expression in androgen-treated VCaP cells. Knocking down ERG by siRNA in VCaP cells enhances PSMA expression both in the presence and absence of synthetic

androgen R1881. Overexpressing *TMPRSS2-ERG* fusions in LNCaP cells downregulated PSMA both in the presence or absence of R1881, while overexpressing wild type ERG did not. Using PSMA-based luciferase reporter assays, we found *TMPRSS2-ERG* fusion can inhibit PSMA activity at the transcriptional level. Our data indicated that down-regulation of PSMA in androgen-treated VCaP cells appears partially mediated by *TMPRSS2-ERG* gene fusion.

Introduction

Prostate specific membrane antigen (PSMA) is a type II transmembrane glycoprotein overexpressed in prostate carcinoma. The protein consists of 750 amino acids with a molecular weight ~ 100 kDa (1). The extracellular domain has activities as a folate hydrolase (cleaving the terminal glutamates from γ-linked polyglutamates) and NAALADase (cleaving the terminal glutamate from α-linked N-acetylaspartyl glutamate). PSMA can undergo internalization, and its intracellular domain is known to bind to actin binding protein filamin A (2, 3). Nearly all prostate cancer cells express PSMA, and its expression has been correlated with aggressive disease (4, 5, 6). In addition to normal prostate gland, benign prostatic hyperplasia (BPH), and prostate cancer (PCa), PSMA is also expressed in the neovasculature of multiple solid tumors (7, 8, 9, 10). Higher PSMA expression is also found in cancer cells from castration-resistant prostate cancer patients. Increased PSMA expression is reported to correlate with the risk of early prostate cancer recurrence after radical prostatectomy. (5, 11, 12). Investigating the mechanism of PSMA regulation will allow us to better understand the mechanisms and functions of PSMA in prostate cancer.

A common genetic alteration in prostate cancer is the presence of the *TMPRSS2-ETS* gene fusion. Studies have shown that a significant fraction of prostate cancers harbor a signature gene fusion between the androgen-regulated *TMPRSS2* and the transformation-specific (ETS) transcription factor family members (13, 14, 15, 16). The *TMPRSS2-ERG* fusion is the most common known gene rearrangement in prostate cancer. Studies found that approximately 50% of prostate cancers harbor *TMPRSS2-ERG* fusions, of which greater than 90% over-express ERG (17). TMPRSS2-ERG fusions alter prostate cancer progression by promoting cell invasion, activating C-MYC oncogene and abrogating prostate epithelial differentiation (15, 18, 19). Recent publications have reported that prostate cancer containing *TMPRSS2-ERG* fusions are significantly enriched for loss of the tumor suppressor PTEN (20). *TMPRSS2-ERG* cooperates with loss of PTEN to further promote prostate cancer progression (20, 21). However, it has been controversial as to whether this fusion product results in increased aggressive behavior in the prostate. While a significant amount of investigations have been done on the tumor biological functions of TMPRSS2 fusion-driven ETS overexpression in prostate cancer, few papers have reported on its potential down-stream targets.

While PSMA is upregulated overall in prostate cancer, it is strongly overexpressed in 50% of prostate cancer specimens. Although *TMPRSS2-ERG* is also found in 50% of prostate cancer specimens, it is unknown if, or to what extent these populations overlap. PSMA is upregulated by androgen ablation, and androgens can stimulate *TMPRSS2-ERG* gene fusion, as the TMPRSS2 promoter has an androgen-responsive element. This information provides a potential link between inhibition of PSMA by androgen and ERG

expression in fusion-positive prostate cancer cells. We hypothesize that PSMA expression could be regulated by the *TMPRSS2-ERG* fusion. VCaP cells express the *TMPRSS2-ERG* fusion, while LNCaP cells do not. Therefore, we investigated PSMA regulation in TMPRSS2-ERG fusion-positive VCaP and fusion-negative LNCaP prostate cancer cells. Our data suggests that down-regulation of PSMA by androgen is mediated by TMPRSS2-ERG gene fusion in VCaP cells.

Materials and Methods

Cell culture and transfection

LNCaP cells (ATCC) were grown in RPMI 1640 medium (Mediatech), and VCaP cells (ATCC) were grown in modified DMEM medium (Cat# 30-2002, ATCC) with 10% fetal bovine serum (USB Corp) in a humidified atmosphere of 5% CO_2 at 37°C. At 60-80% confluence cell lines were incubated with vehicle DMSO or 10 μM flutamide (androgen receptor antagonist; Sigma) for 2 hours before treatment with 5 nM of R1881 (synthetic androgen, Perkin Elmer) for 24 hours. *TMPRSS2-ERG* fusion transcript isoforms (III, III+72, VI, VI+72) (18) or ERG cDNA (RC218892, OriGene Technologies, Inc.) were transfected into LNCaP cells by Lipofectamine 2000 (Cat# 11668-019, Invitrogen). The empty vectors were pcDNA3.1 and pCMV6-Entry respectively. Transfections were performed according to the manufacturer's instruction (Invitrogen). The ratio of DNA (μg) to Lipofectamine 2000 (μl) is 1:2.5. Expression of ERG fusion proteins and wild type ERG were checked by western blot.

ERG knockdown with small interfering RNA (siRNA)

For siRNA knockdown of ERG, siRNA against human ERG (NM_004440) was designed as 5'-GACATCCTTCTCTCACAT-3' (Ambion, Austin, TX) or purchased from Dharmacon (D-001210-01; Lafayette, CO). They are designated as siERG-1 (from Ambion) and siERG-2 (from Dharmacon) respectively. Negative control #1 siRNA (Cat#4390843; Ambion) or siRNA against ERG was transfected into VCaP cells as indicated, using Oligofectamine (Cat# 12252-011, Invitrogen). Transfections were performed according to the manufacturer's instruction (Invitrogen). VCaP cells were seeded into 12-well plate one day before transfection. 200 nM of siRNA and 3 μl of Oligofectamine were used for each transfection. After 24 hours, a second identical transfection was carried out and cells were harvested 24 hour later. siRNA knockdown of ERG was tested by both quantitative polymerase chain reaction (qPCR) or immunoblot analysis. Experiments were done in triplicate.

Detection of proteins by Western Blot analysis

Cells were lysed in RIPA buffer (50 mM Tris-HCl, pH7.5, 150 mM NaCl, 1% Igepal CA-630, 0.5% Na Deoxycholate, 0.1% SDS, 1 mM EDTA, 50 mM NaF, 200 μM Na Orthovanadate) supplemented with protease inhibitor cocktail (Cat# 11836153001, Roche). Protein samples were run in 7.5% Tris-HCL precast ready gel (Cat# 161-1154, BIO-RAD) and transferred into PVDF membrane. Blots were blocked in 5% skim milk and incubated with anti-ERG antibody (1: 1000 dilution) (Cat# sc-354, Santa Cruz Biotechnology), anti-PSMA antibody GCP-04 (1:10000 dilution) (gift from Dr. Jan Konvalinka, Academy of Sciences of the Czech Republic, Prague, Czech Republic), anti-V5 antibody (1: 1000 dilution) (Cat# R961-25, Invitrogen), or anti-

GAPDH (1: 20000 dilution) (Cat# 2-RGM2, Advanced ImmunoChemical Inc.). HRP labeled goat anti-rabbit or goat anti-mouse was used as secondary antibody (1:5000; Pierce). Signal was detected by chemiluminescent substrate from Pierce (Cat# 34080).

Real-Time RT-PCR analysis

Gene expression was verified by real-time reverse transcription (RT)-PCR. The first strand of cDNA was synthesized from RNA samples with an iScript cDNA synthesis kit (Cat# 170-8890, Bio-Rad Laboratories). 500 ng of total RNA from each sample was applied to each reaction. 20 µL of complete reaction mix was incubated at 25 ºC for 5 min, followed by 42 ºC for 30 min and 85 ºC for 5 min. After cDNA synthesis, 2 µL of reaction was then used to set up PCR reactions with an iQ SYBR Green Supermix kit (Cat# 170-8882, Bio-Rad). Total reaction volume for PCR was set to 20 µL in 2x SYBR Green Supermix with gene specific primers. Reactions were run at 95 ºC for 10 sec, 60 ºC for 30 sec followed by 40 cycles. Fluorescent data were collected in an iCycler iQ detection system (Bio-Rad). For each sample in a given experiment, duplicate reactions were set up with a primer pair for the gene of interest, as well as duplicate reactions with a primer pair for phosphogluconate dehydrogenase (PGD), which was used as an endogenous reference. Using the comparative threshold cycles (CT) method, the quantification normalized to PGD and relative to untreated, parental cells was performed. Fold changes were calculated using the formula $2^{-\Delta\Delta CT}$, where ΔCt is $Ct_{(target\ gene)}$-$Ct_{(PGD)}$, $\Delta\Delta Ct$ is $\Delta Ct_{(treatment)}$- $\Delta Ct_{(control)}$. Experiments were done in triplicate. Primer sets: PSMA forward: 5'-TCTGCTCGCGCCGAGATGTG-3'; PSMA reverse: 5'-ATTTTATAAACCACCCGAAG-3'; TMPRSS2/ERG forward: 5'-TAGGCGCGAGCTAAGCAGGAG-3'; TMPRSS2/ERG reverse: 5'-ACGCGGTCATCTGTGTCTTA-3'; PGD forward: 5'-AGACCATCTTCCAAGGCATTG-3'; PGD reverse: 5'-GTGGTATGCCTCACAGATCAG-3'.

Luciferase reporter assay

VCaP cells were transfected with plasmid for PSM-Luc (contains PSMA promoter and enhancer) and Renilla-Luc luciferase reporter genes. Twenty-four hours post-transfection, cells were cultured in DMEM medium containing 9% charcoal-stripped fetal bovine serum (C-FBS, Hyclone) +1% normal FBS, and cultured for another 24 hours in the presence or absence of R1881, flutamide, or bicalutamide. Prior to harvest, LNCaP cells were co-transfected with TMPRSS2-ERG fusion transcript isoforms and PSM-Luc and Renilla-Luc. Twenty-four hours post-transfection, cells were cultured in phenol red-free RPMI 1640 (Invitrogen) containing 9% charcoal-stripped serum (CSS) +1% normal serum, and cultured for another 24 hours in the presence or absence of R1881. Cells were harvested, and firefly and *Renilla* luciferase activities were measured using the Dual-Luciferase Reporter Assay System according to the manufacturer's instruction (Promega).

Chromatin Immunoprecipitation

Chromatin immunoprecipitation (ChIP) was performed by using a ChIP kit according to the manufacturer's instructions (ab500, Abcam Inc.). In brief, about $3x10^6$ VCaP cells were fixed in 37% formaldehyde before lysis. Chromsomal DNA was sheared by using

a sonicator to an optimal DNA fragment size of 200-1000 bp. Anti-ERG (sc-354, Santa Cruz) antibody was used in the immunoprecipitation to pull down ERG protein and DNA complex. Rabbit IgG was used as negative control. After DNA purification, 0.5 ul each of input DNA, ERG-enriched, or rabbit IgG-enriched DNA were subjected to PCR analysis. A 192 bp fragment of PSMA promoter was amplified by the upstream 5'-TGCACGGCCTCTCTCACGGA-3' and downstream 5'-GGCTATGTCTGGCTACTGTCTTA-3' primers.

Statistical analysis

For real-time PCR, the ΔCt values of treatment groups and vehicle control were compared using 2-sided paired t-tests which blocked on experimental replicates. For the luciferase assay, we analyzed data by using two sample t-test due to the pooled nature of the experiment. Significance was accepted when $p<0.05$.

Results

Inhibition of PSMA expression by the nonaromatizable androgen R1881 in VCaP cells. Both VCaP and LNCaP cells were treated with vehicle or the androgen antagonist flutamide prior to treatment with the synthetic androgen R1881. After 24 hours treatment, TMPRSS2-ERG mRNA and protein levels were induced in VCaP cells by R1881, and the increased expression was attenuated by the addition of flutamide (Fig. 1A). PSMA mRNA levels dramatically decreased in VCaP cells (Fig. 1B), while a modest decrease was observed in LNCaP cells after R1881 exposure for 24 hours (Fig. 3A). Treatment with flutamide partially restored PSMA mRNA level (Fig. 1B). After R1881 treatment for 3 days, PSMA protein levels were also decreased in VCaP cells (Fig. 1C). Since PSMA protein has a long half life, it took a longer time to decrease its protein level than to decrease mRNA level by R1881. Reports have shown PSMA is up-regulated by androgen ablation (12); however, we found that the response of PSMA to androgen treatment was different in VCaP and LNCaP prostate cancer cell lines. R1881 significantly reduces PSMA in VCaP cells while it has a modest decrease in LNCaP cells. Interestingly, we found AR mRNA levels in response to its ligand were also different in these two cell lines. AR mRNA is dramatically reduced by R1881 in VCaP cells, while it has minimal change in LNCaP cells (data not shown). Our result is consistent with Makkonen's findings published recently (29). VCaP cells harbor the *TMPRSS2-ERG* fusion and contain wild type AR, while LNCaP cells lack this fusion gene and have a mutated AR. Therefore, it is possible that the differential inhibition of PSMA by androgen treatment in VCaP cells and LNCaP cells is due to either the TMPRSS2-ERG fusion or the different type of AR. Moreover, AR expression level is higher in VCaP cells than in LNCaP cells, and the pattern for regulation of AR target gene expression by amplification of AR is also different in these two cell lines (29).To clarify this point, we further determined PSMA expression following siRNA knock down of ERG in VCaP cells.

ERG knockdown enhances PSMA expression in VCaP cells. It is reported the TMPRSS2-ERG fusion transcripts encode truncated ERG proteins at the amino terminus (19) and the vast majority of total ERG mRNA represents fusion gene transcripts. Therefore, by knocking down ERG, we can effectively evaluate the function of the TMPRSS2-ERG fusions. VCaP cells were transfected with siRNA for 3 days. Knocking down ERG was verified by real-time PCR. ERG mRNA level was reduced by 50% using specific ERG siRNA (Fig. 2A). Further knocking down of ERG was achieved by using combination of two siRNA siERG-1 and siERG-2 (Fig. 2A). Partially silencing of ERG alone can enhance PSMA expression in VCaP cells (Fig. 2B, 2C). When treated with R1881, low PSMA expression was partially restored in ERG knockdown VCaP cells (Fig. 2B). These data indicate that either or both of the TMPRSS2-ERG fusion or wild type ERG can suppress PSMA expression in VCaP cells. To verify what type of ERG was involved in PSMA expression, next we checked their effects by overexpressing TMPRSS2-ERG fusion or wild type ERG in LNCaP cells.

Overexpression of TMPRSS2-ERG fusions decreased PSMA expression in LNCaP cells. TMPRSS2-ERG fusion isoforms have variable biological activities (18). Of the fusion isoforms, the most common transcripts are type III (TMPRSS2 exon 1 fused to ERG exon 4) and type VI (TMPRSS2 exon 2 fused with ERG exon 4). Type III encodes a truncated ERG protein, while type VI encodes a true fusion protein (18). Recently a 72-bp exon was found in some alternatively spliced fusion isoforms. The presence of 72 bp exon has a significant biological function in cell proliferation (18). Both of the type III+72 and type VI+72 isoforms can enhance cell proliferation. To further identify whether inhibition of PSMA is mediated by wild type ERG or by different TMPRSS2-ERG fusions, we transfected these ERG fusion constructs into LNCaP cells, which is ERG fusion-negative. When LNCaP cells were transfected with TMPRSS2-ERG fusion constructs, ERG fusion proteins were detected by using anti-V5 antibody (Fig. 3B). We found PSMA was downregulated, and its suppression was enhanced in the presence of R1881 (Fig. 3C). On the other hand, when LNCaP cells were transfected with normal ERG (Accession No: NM_004449.3), no change in PSMA expression was observed in this cell line. (Fig. 3D, 3E). When treated with R1881, which can partially inhibit PSMA expression, the extent of inhibition was to the same extent both in the presence or absence of ERG (Fig. 3E). Given that the transfection efficiency in LNCaP cells is only around 50% by Lipofectamine (data not shown), and that we only found partial inhibition of PSMA in LNCaP cells by transient transfection of TMPRSS2-ERG fusions, more complete inhibition of PSMA expression would likely to be achieved with a higher transfection efficiency. We did not see any different effect on PSMA inhibition among the different types of alternate TMPRSS2-ERG transcripts. Our data suggests that inhibition of PSMA by androgen in VCaP cells may be mediated by truncated ERG or fusion proteins that are encoded by *TMPRSS2-ERG*, not by normal ERG protein.

Inhibiton of PSMA luciferase activity by TMPRSS2-ERG. According to MAT inspector software (http://www.genomatix.de/index.html), we found potential ETS transcription binding sites on the PSMA promoter and enhancer (data not shown). One of these binding sites on the PSMA promoter (nt 943-963) was highly conservative, according to computational prediction (http://genome.ucsc.edu/index.html; http://weblogo.berkeley.edu/) (Fig. 4A). We hypothesized that TMPRSS2-ERG can

regulate PSMA at the transcription level. Therefore, we performed a ChIP assay and also transfected a luciferase reporter gene that contains the PSMA promoter and enhancer sequences into both VCaP and TMPRSS2-ERG-transfected LNCaP cells or its derivative cell line, C4-2. Recruitment of ERG to the *PSMA* promoter in VCaP cells was detected by ChIP assay (Fig. 4A). PSMA luciferase activity was inhibited in VCaP cells when treated with R1881 for 24 hours. Flutamide can reverse this inhibition (Fig. 4B). LNCaP and C4-2 cells that were cotransfected with TMPRSS2-ERG fusion isoforms and the PSMA luciferase reporter gene showed that different TMPRSS2-ERG isoforms alone can inhibit PSMA transcription activity, and the activity was further inhibited by R1881 treatment (Fig. 4C and 4D). These data confirm that TMPRSS2-ERG fusion can inhibit PSMA expression at the transcription level.

Discussion

Increased PSMA expression has been correlated with a high Gleason score of disease and with tumor recurrence in prostate cancer. In this study, we found PSMA was down-regulated by *TMPRSS2-ERG* fusion in VCaP prostate cancer cells after androgen stimulation. This is the first data to identify the mechanism for the androgen signaling pathways involved in PSMA regulation. Recent reports indicate that the *TMPRSS2-ERG* fusion gene was present and expressed in pre-surgery androgen ablation patients (22). In addition, ERG was found in circulating tumor cells from patients with castration-resistant prostate cancer (23). Androgen ablation inhibits the expression of *TMPRSS2-ERG*. Moreover, patients with expression of the fusion gene had earlier prostate specific antigen (PSA) recurrence after radical prostatectomy (22). Our findings demonstrate that in VCaP cells TMPRSS2-ERG fusions, but not wild type ERG, suppress PSMA expression. As there is an inverse relationship between PSMA expression and ERG fusions, it seems unlikely that studies claiming high expression of PSMA correlates to higher percentage and earlier failure of PSA would also be occurring in those the TMPRSS-ERG protein is expressed. Developing results from ongoing studies of prostate tissue microarrays demonstrated a negative correlation between PSMA expression and ERG expression in Gleason Score 7 prostate cancer (communication with Dr. Magi-Galluzzi Cristina from Cleveland Clinic), which is consistent with our *in vitro* findings.

Androgen signaling is important for prostate cancer growth and survival. Androgen exerts its biological functions through binding to the AR (24). Overexpression of AR was found in castration-resistant prostate cancer (25, 26). Investigators reported that high levels of AR in androgen deprivation therapy down-regulated *TMPRSS2-ERG* fusion. The fusion gene can be up-regulated at a late time by reactivating AR in castration-resistant prostate cancer (27). Also, ERG can disrupt AR signaling by inhibiting AR expression (28). In our study, we found that PSMA could be a potential downstream target of *TMPRSS2-ERG* fusion in the AR signaling pathway. Since there is a correlation between AR and TMPRSS2-ERG expression, more work needs to be done to further address the role of AR in ERG fusion mediated PSMA expression.

We observed that PSMA regulation by androgen could be mediated by the *TMPRSS2-ERG* fusion. Knocking down mutant ERG can increase PSMA expression. This finding suggests that in men with prostate cancers bearing the TMPRSS2-ERG fusion that a short course of androgen ablation might upregulate PSMA and facilitate therapeutic targeting and/or imaging based on PSMA.

The androgen receptor remains an important target. Androgen synthesis inhibitors and new more effective antiandrogens are demonstrating encouraging responses in castrate resistant disease. Still these therapies will also eventually develop resistance and other non-androgen based therapies such as linked toxin targeting may add to the arsenal of therapeutic agents available for treatment. Since PSMA is a promising target for prostate cancer therapy and imaging, further elucidation of the relationship between *TMPRSS2* gene fusions and PSMA could reveal novel pathways for enhancing targeted prostate cancer treatment.

Competing interests

No competing interests exist.

Acknowledgments

Grant support: This work was supported by grants from NIH CA101069, WDWH and from the Department of Defense Prostate Cancer Research program DAMD-W81XWH-09-1-0385, MI.

We also like to thank Drs. Lisa Middleton, Charles Foster and Yongzhong Zhao from the Department of Cancer Biology at Cleveland Clinic for their helpful criticism of the manuscript. Kelley Harsch is thanked for her technical support.

References

1. Israeli RS, Powell CT, Corr JG, et.al. (1993) Molecular cloning of a complementary DNA encoding a prostate-specific membrane antigen. Cancer Res 53: 227-230.
2. Liu H, Rajasekaran AK, Moy P, et.al. (1998) Constitutive and antibody-induced internalization of prostate-specific membrane antigen. Cancer Res 58: 4055-4060.
3. Anilkumar G, Rajasekaran SA, Wang S, et.al. (2003) Prostate-specific membrane antigen association with filamin A modulates its internalization and NAALADase activity. Cancer Res 63: 2645-2648.
4. Tasch J, Gong M, Sadelain M, et.al. (2001) A unique folate hydrolase, prostate-specific membrane antigen (PSMA): A target for immunotherapy? Crit Rev Immunol 21: 249-261.
5. Ross JS, Sheehan CE, Fisher HAG, et.al. (2003) Correlation of primary tumor prostate-specific membrane antigen expression with disease recurrence in prostate cancer. Clin Cancer Res 9: 6357-462.
6. Perner S, Hofer MD, Kim R, et.al. (2007) Prostate-specific membrane antigen expression as a predictor of prostate cancer progression. Hum Pathol 38: 696-701.
7. Liu H, Moy P, Kim S, et.al. (1997) Monoclonal antibodies to the extracellular domain of prostate-specific membrane antigen also react with tumor vascular endothelium. Cancer Res 57: 3629-34.
8. Chang SS, Reuter VE, Heston WD, et.al. (1999) Five different anti-prostate specific membrane antigen (PSMA) antibodies confirm PSMA expression in tumor-associated neovasculature. Cancer Res 59 (13): 3192-8.

9. O'Keefe DS, Bacich DJ, Heston WD. (2004) Comparative analysis of prostate-specific membrane antigen (PSMA) versus a prostate-specific membrane antigen-like gene. Prostate 58: 200-10.

10. HAFFNER MC, KRONBERGER IE, ROSS JS, ET.AL. (2009) PROSTATE-SPECIFIC MEMBRANE ANTIGEN EXPRESSION IN THE NEOVASCULATURE OF GASTRIC AND COLORECTAL CANCERS. HUM PATHOL 40 (12): 1754-61.

11. Mitsiades CS, Lembessis P, Sourla A, Milathianakis C, et.al. (2004) Molecular staging by RT-PCR analysis for PSA and PSMA in peripheral blood and bone marrow samples is an independent predictor of time to biochemical failure following radical prostatectomy for clinically localized prostate cancer. Clin Exp Metastasis 21: 495-505.
12. Wright GL Jr, Grob BM, Haley C, Grossman K, Newhall K, Petrylak D, Troyer J, Konchuba A, Schellhammer PF, Moriarty R. (1996) Upregulation of prostate-specific membrane antigen after androgen-deprivation therapy. Urology 48(2): 326-334.
13. Tomlins S, Rhodes DR, Perner S, et.al. (2005) Recurrent fusion of *TMPRSS2* and ETS transcription factor genes in prostate cancer. Science 310: 644-648.
14. Tomlins SA, Mehra R, Rhodes DR, et.al. (2006) TMPRSS2:ETV4 gene fusions define a third molecular subtype of prostate cancer. Cancer Research 66 (7): 3396-3400.
15. Tomlins SA, Laxman B, Varambally S, et.al. (2008) Role of *TMPRSS2-ERG* gene fusion in prostate cancer. Neoplasia 10 (2): 177-188.
16. Perner S, Demichelis F, Beroukhim R, et.al. (2006) *TMPRSS2:ERG* fusion-associated deletions provide insight into the heterogeneity of prostate cancer. Cancer Research 66 (17): 8337-8341.
17. Demichelis F, Fall K, Perner S, et.al. (2007) TMPRSS2:ERG gene fusion associated with lethal prostate cancer in a watchful waiting cohort. Oncogene 26: 4596-4599.
18. Wang J, Cai Y, Yu W, et.al. (2008) Pleiotropic biological activities of alternatively spliced TMPRSS2-ERG fusion gene transcripts. Cancer Research 68: (20): 8516-8524.
19. Sun C, Dobi A, Nohamed A, et.al. (2008) TMPRSS2-ERG fusion, a common genomic alteration in prostate cancer activates C-MYC and abrogates prostate epithelial differentiation. Oncogene 27: 5348-5353.
20. Carver BS, Tran J, Gopalan A, et.al. (2009) Aberrant ERG expression cooperates with loss of PTEN to promote cancer progression in the prostate. Nature Genetics 41 (5): 619-623.
21. King JC, Xu J, Wongvipat J, et.al. (2009) Cooperativity of *TMPRSS2-ERG* with PI3-kinase pathway activation in prostate oncogenesis. Nature Genetics 41 (5): 524-526.

22. Bonaccorsi L, Nesi G, Nuti F, et.al. (2009) Persistence of expression of the TMPRSS2:ERG fusion gene after pre-surgery androgen ablation may be associated with early prostate specific antigen relapse of prostate cancer: preliminary results. J Endocrinol Invest 32 (7): 590-6.
23. Attard G, Swennenhuis JF, Olmos D, et.al. (2009) Characterization of ERG, AR and PTEN gene status in circulating tumor cells from patients with castration-resistant prostate cancer. Cancer Res 69 (7): 2912-2918.
24. Heinlein CA, Chang C. (2004) Androgen receptor in prostate cancer. Endocr Rev 25: 276-308.
25. Hu R, Dunn TA, Wei S, et.al. (2009) Ligand-independent androgen receptor variants derived from splicing of cryptic exons signify hormone-refractory prostate cancer. Cancer Res 69 (1): 16-22.
26. Waltering KK, Helenius MA, Sahu B, et.al. (2009) Increased expression of androgen receptor sensitizes prostate cancer cells to low levels of androgens. Cancer Res 69 (20): 8141-8149.
27. Cai C, Wang H, Xu Y, et.al. (2009) Reactivation of androgen receptor-regulated TMPRSS2:ERG gene expression in castration-resistant prostate cancer. Cancer Res 69 (15): 6027-6032.
28. Yu J, Yu J, Mani R, Cao Q, et. al. (2010) An integrated network of androgen receptor, polycomb, and TMPRSS2-ERG gene fusions in prostate cancer progression. Cancer Cell 17: 443-454.
29. Makkonen H, Kauhanen M, Jaaskelainen T, Palvimo JJ. (2011) Androgen receptor amplification is reflected in the transcriptional responses of Vertebral-Cancer of the prostate cells. Molecular and Cellular Endocrinology (331): 57-65.

Figure legends

Figure 1. Inhibition of PSMA by androgen in VCaP cells. A, Expression levels of TMPRSS2-ERG in VCaP cells by real-time PCR, normalized to PGD mRNA level. ERG protein level was measured by western blot after treatment with 5 nM of R1881 or 10 μM of antagonist flutamide for 1 day. B, PSMA expression was detected by real-time PCR in VCaP cells, normalized to PGD. (Cells were treated the same as in Fig 1A). C, PSMA protein levels were checked by western blot in VCaP cells treated with 5 nM of R1881 for 0-5 days. For real-time PCR, cells were treated with vehicle or androgen antagonist flutamide for 2 hours prior to the treatment of the synthetic androgen R1881 for 24 hours. Experiments were done in triplicate.

Figure 2. Knocking down ERG by siRNA enhances PSMA expression in VCaP cells. A, Cells were transfected with different ERG siRNA by oligofectamine for 48 hours. ERG expression levels were tested by quantitative real-time PCR, normalized to PGD mRNA level. B, Real-time PCR for PSMA expression in ERG knockdown VCaP cells. Cells were treated with or without R1881 for 24 hours after 48 hours treatment of siRNA. C, Western blot for ERG and PSMA expression in ERG knockdown VCaP cells. Cells were harvested 72 hours post siRNA transfection.

Figure 3. Overexpression of *TMPRSS2-ERG* fusions decreased PSMA expression in LNCaP cells. A, PSMA expression was detected by real-time PCR in LNCaP cells, normalized to PGD mRNA level. Cells were treated with vehicle DMSO or androgen antagonist flutamide for 2 hours prior to the treatment of the synthetic androgen R1881 for 24 hours. B, TMPRSS2-ERG fusion protein levels were checked by Western blot using anti-V5 antibody. LNCaP cells were transfected with fusion type III, III+72, VI, VI+72, or empty vector for 48 hours. C, Real-time PCR detected PSMA mRNA level in TMPRSS2-ERG fusion-transfected LNCaP cells. Cells were transfected with fusions or empty vector for 48 hours, then treated with or without R1881 for 24 hours. D, ERG expression level in ERG-transfected LNCaP cells by western blot. Cells were transfected with full length ERG for 48 hours. E, PSMA mRNA level in ERG overexpressing LNCaP cell. Cells were treated with or without R1881 for 24 hours post 48 hours of transfection. Experiments were done in triplicate.

Figure 4. PSMA luciferase activity in VCaP or LNCaP cells. A, Graphic prediction of ETS transcription factor binding site on PSMA promoter and recruitment of ERG to PSMA promoter detected by ChIP assay. B, PSMA luciferase activity in VCaP cells. VCaP cells were transfected with PSM-Luc and Renilla-Luc luciferase reporter genes for 24 hours, then cells were treated with R1881 and androgen antagonist flutamide for another 24 hours. C and D, PSMA luciferase activity in LNCaP and C4-2 cells. LNCaP and C4-2 cells were co-transfected with PSM-Luc, Renilla-Luc, and TMPRSS2-ERG fusions, type III, III+72, VI, VI+72. Twenty-four hours post transfection, cells were cultured in the presence or absence of R1881 for another 24 hours.

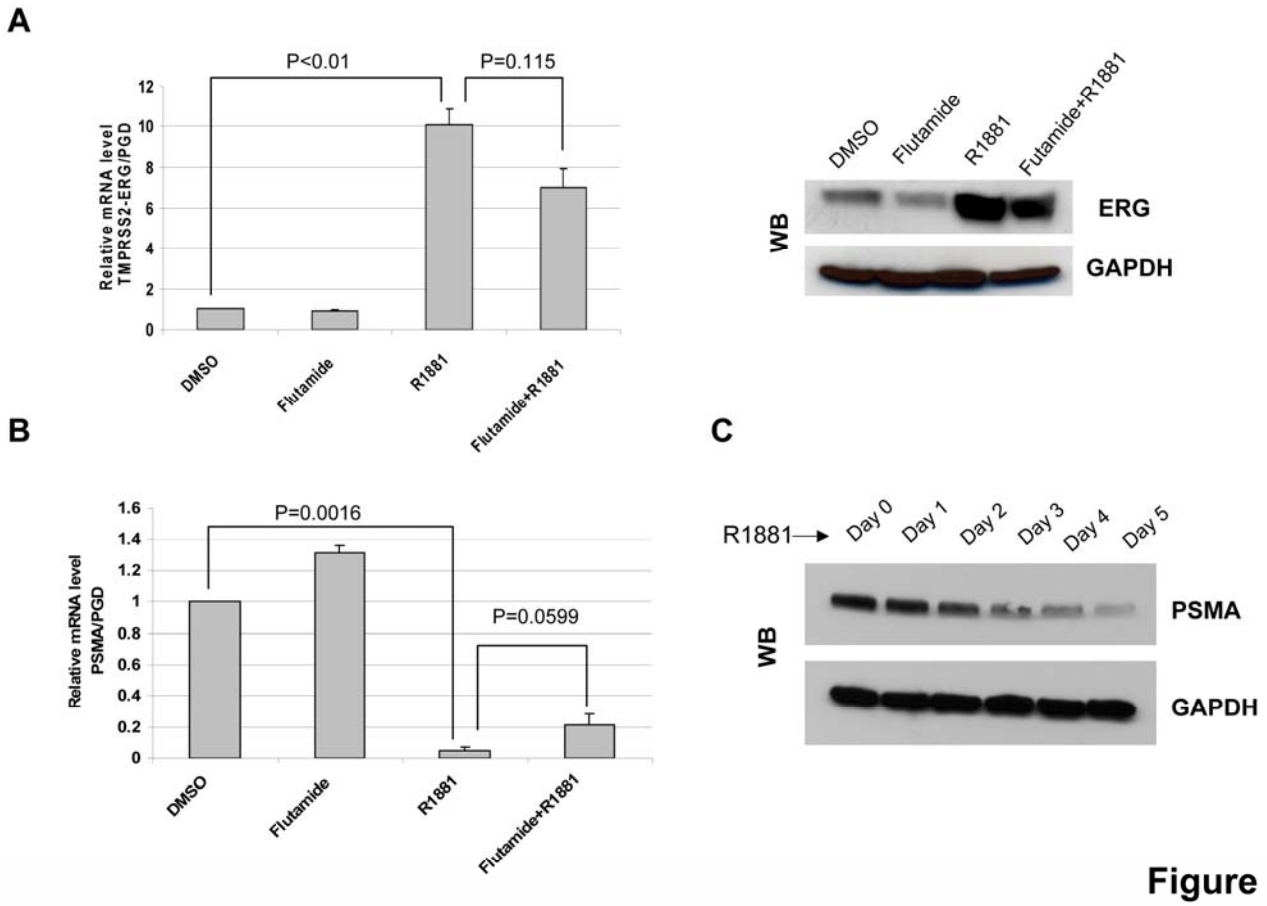

Figure 1

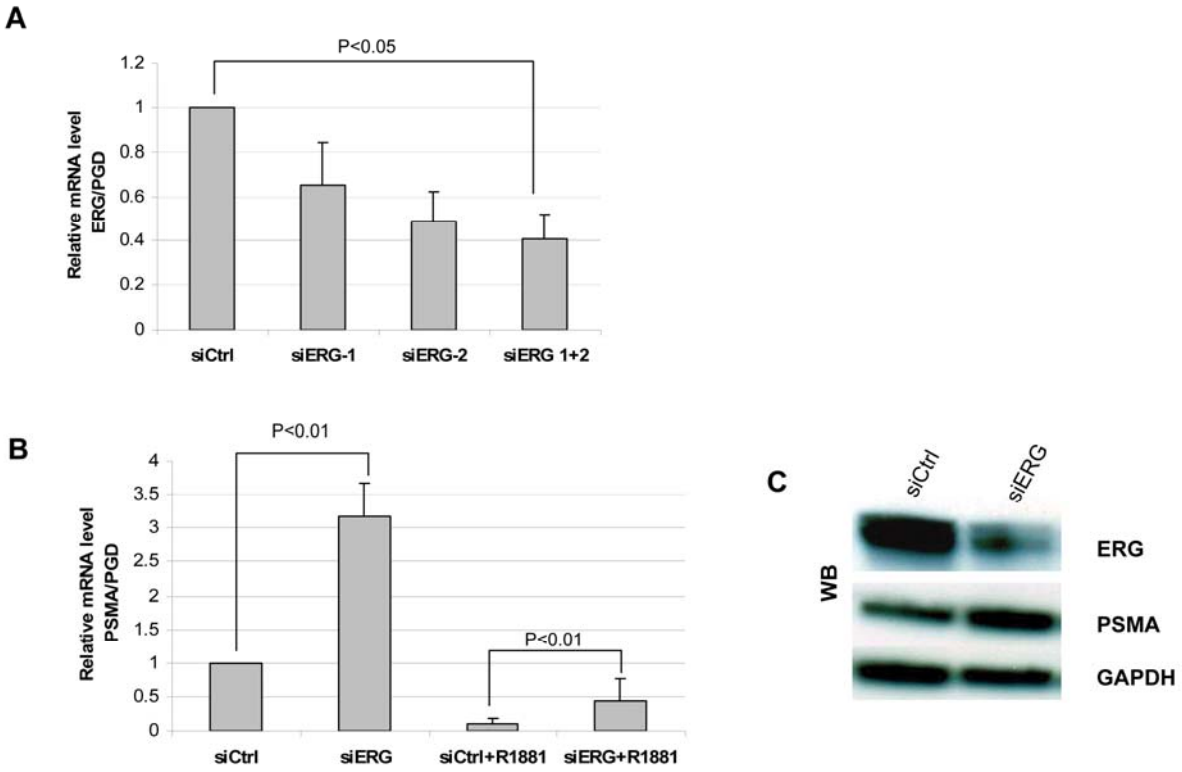

Figure 2

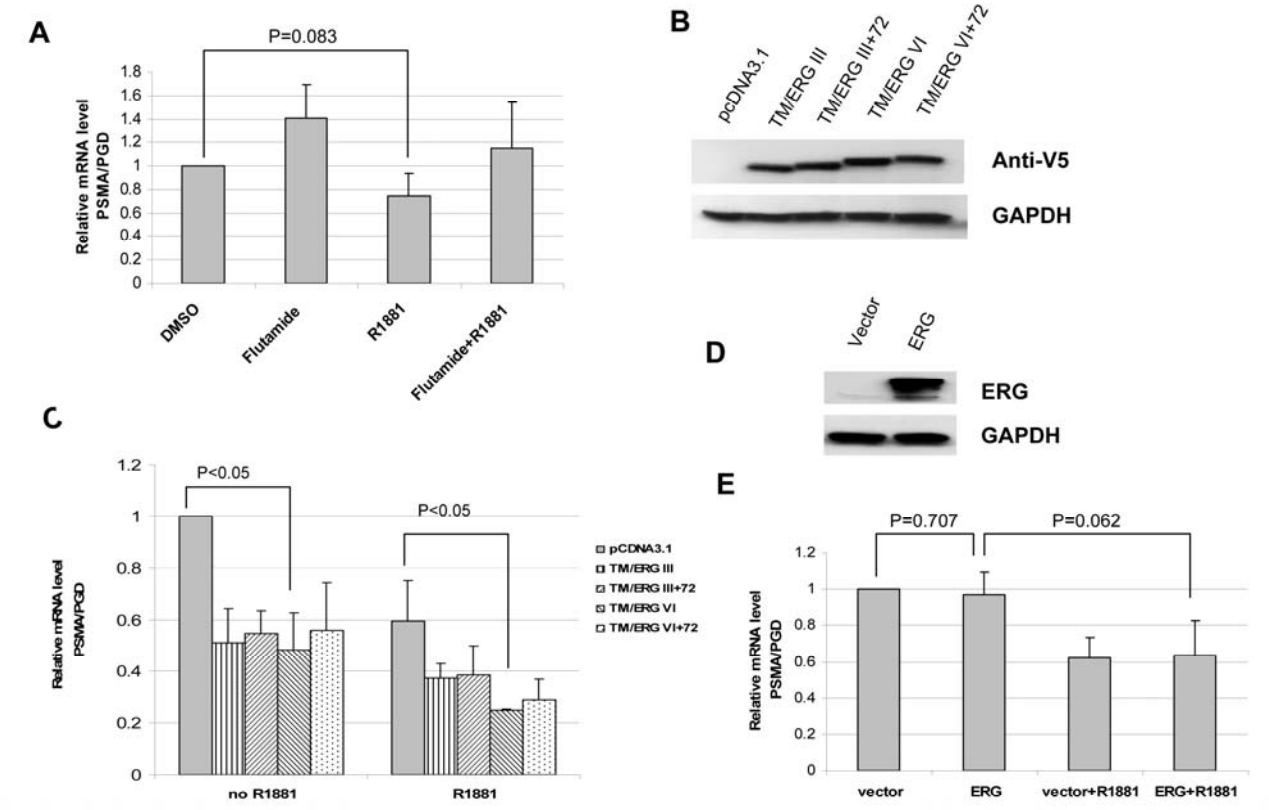

Figure 3

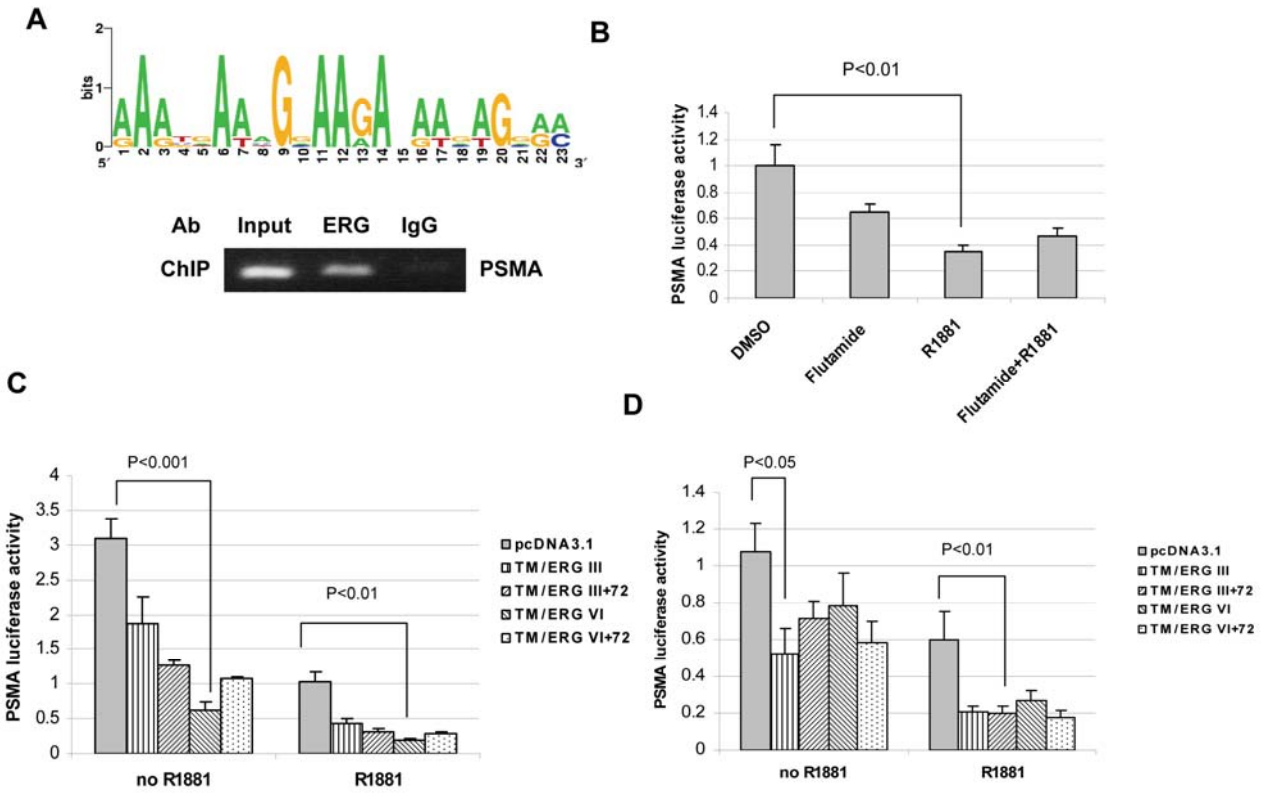
A
bits
Ab
Input
ERG
IgG
ChIP
PSMA
B
P<0.01
PSMA luciferase activity
DMSO
Flutamide
R1881
Flutamide+R1881
C
P<0.001
P<0.01
PSMA luciferase activity
no R1881
R1881
pcDNA3.1
TM/ERG III
TM/ERG III+72
TM/ERG VI
TM/ERG VI+72
D
P<0.05
P<0.01
PSMA luciferase activity
no R1881
R1881
pcDNA3.1
TM/ERG III
TM/ERG III+72
TM/ERG VI
TM/ERG VI+72

Figure 4

(Submitted for publication)

Synthesis and Biological Evaluation of New Ligands for Future Imaging of Prostate Cancer by Targeting Prostate Specific Membrane Antigen (PSMA)

Xinning Wang[1], Haibin Tian[2], Zhenghong Lee[2], Warren D.W. Heston[1,*]

[1] Department of Cancer Biology, Cleveland Clinic, 9500 Euclid Ave, Cleveland OH, 44195

[2] Department of Radiology, Case Western Reserved University

* To whom correspondence should be addressed. Phone: 216-444-8181. Fax: 216-445-0610. E-mail: hestonw@ccf.org. Address: Warren D.W. Heston, Cleveland Clinic, 9500 Euclid Ave, Cleveland, OH, 44195.

Abbreviations: PSMA, prostate specific membrane antigen; ^{3}H-ZJ24, N-[N-[(*S*)-1,3-dicarboxypropyl]carbamoyl]-*S*-[^{3}H]-methyl-L-cysteine; SMCC, Succinimidyl 4-(N-maleimidomethyl)cyclohexane-1-carboxylate; SFB, N-succimimidyl 4-fluorobenzoate; $MTXGlu_2$, 4-amino-10-methylpteroyldi-γ-L-glutamic acid; MTX, methotrexate; Rt, retention time; r.t., room temperature

Abstract

Prostate specific membrane antigen (PSMA) is a type II transmembrane protein that is highly expressed in prostate cancer. It is an ideal biomarker for diagnosis and therapy of prostate cancer. A previously reporte compound RBI1033 showed binding affinity more than 10 time higher than the parent urea-based compound. The purpose of this work is to further explore the structure-activity relationship of RBI1033 to help identify highly selective ligands of PSMA. By chemically linking amine-containing molecules to PSMA recognizing dipeptide Cys-C(O)-Glu through a 4-(N-maleimidomethyl) cyclohexane-1-amidate linkage, a series of RBI1033 analogues have been synthesized. Interestingly, it was found that ligands having 2-5A in their structure showed extraordinary improved binding and inhibitory activity to PSMA compared to parent ligand Cys-C(O)-Glu. Removing of 2-5 reduced their biological activity. Therefore, integration of 2-5A in the structure plays an important role in improving the binding affinity to PSMA. Furthermore, the ligands reported here can be easily radiolabel for future PET imaging of prostate cancer. The results of these experiments will provide a path to agents that will be synthetically achievable and likely be more cost effective than current antibody-based methods.

Introduction

According to the American Cancer Society, prostate cancer is the most prevalent cancer in American males and represents their second leading cause of cancer death. Prostate cancer kills more than 200,000 men annually worldwide. About 192,280 new cases of prostate cancer will be diagnosed, and about 27,360 men will die of the disease in the United States in 2009.[1] While prostate specific antigen (PSA) is a useful serum marker for prostate cancer, changes in PSA levels may reflect the impact of therapy on PSA expression instead of actual tumor size making it difficult to evaluate the response to chemotherapy. Another problem is that prostate cancer metastasizes to bone, and tumor volume in bone is difficult to evaluate. More accurate staging would facilitate treatment decisions and lead to a better outcome for patients. Particularly useful would be an imaging technique that could be correlated with a relevant tumor biomarker.

Prostate specific membrane antigen (PSMA) was originally discovered in the androgen-dependent LNCaP human prostate adenocarcinoma cell lines by mAb 7E11C-5.3.[2] PSMA is a type II transmembrane protein consisting of 750 amino acids and having a molecular weight of ~110,000.[3, 4] Immunohistochemical analysis of pathological specimens indicates that PSMA is expressed by virtually all prostate cancers, and its expression is further increased in poorly differentiated, metastatic, and hormone-refractory carcinomas.[3, 5, 6] PSMA expression has also been found in a variety of tumor, but not normal, vascular endothelium, which further broadens its interest and potential applications in anti-angiogenic therapies.[7, 8] In contrast to other well-known prostate-restricted molecules such as PSA that are secretory proteins, PSMA is a type II integral cell-surface membrane protein that is not secreted.[7] With its abundant expression in most prostate cancers, PSMA would therefore appear to be an ideal target for diagnosis and therapy. A radiolabeled form of the antibody 7E11 (ProstaScint) is used clinically to image and stage prostate cancer, validating the utility of PSMA for tumor targeting.[9] However this imaging agent binds to an intracellular portion of PSMA and thus is likely imaging sites of tumor necrosis and its use has been limited.

To target viable tumor cells, second generation antibodies such as the humanized version of J591 have been developed.[10] The results of these second generation antibodies are encouraging and are demonstrating therapeutic activity in delivering radionuclides and cytotoxic agents in both preclinical and early clinical trails.[11-14] For example, Antibody MLN 591 (formerly J591) is presently in clinical trials, linked to radiometals as imaging reagent and to cytotoxins as therapeutic agent.[15-19] Despite these positive results, there are some restrictions of the mAb-targeted imaging, such as biochemical and biological instability of the mAbs and poor extravascular diffusion. Use of small molecules, which have high affinity to PSMA, can overcome those obstacles.

The development of small molecules as potential imaging agents has been based on the identification of enzymatic activity of PSMA. It cleaves alpha-linked glutamates from N-acetylaspartylglutamate.[20] PSMA also has a unique folate hydolase activity which

can remove the gamma-linked terminal glutamates from folate in a sequential fashion.[21] Highly potent ligands targeting PSMA have been described recently.[22-26] To date some of the best low weight inhibitors are highly charged water soluble agents which include as part of their structure the di-acid of glutamic acid. One of the leading compounds is (S)-2-(3-((S)-5-amino-1-carboxypentyl)ureido)pentanedioic acid (Cys-CO-Glu, **1**, Figure 1) containing a central urea group.[27] It can be easily modified without compromising activity through the –SH group. Selective imaging of PSMA-expressing tumor xenografts has been reported by radiolabeling of the urea-based PSMA inhibitors.[28-33] These reports encouraged us to develop new urea-based analogues that have better binding affinity and can be feasibly radiolabeled for diagnose of prostate cancer. Recently, an 2-5A containing urea-based analogue **RBI1033** (Figure 1) has been synthesized, which showed binding activity 10 times better than compound **1** itself.[34] Therefore, the purpose of this study is to perform structure-activity relationship studies of **RBI1033** to help identify highly selective inhibitors of the enzymatic activity of membrane associated PSMA that can be subsequently coupled to imaging agents for systemic delivery to localized, primary and disseminated, metastatic prostate tumors.

Results

Chemistry

SMCC is a heterobifunctional linker. It can covalently conjugate to amine- and sulfhydryl-containing molecules through its N-hydroxysuccinimide (NHS) ester and maleimide group. Hydrolysis of NHS ester competes with reaction in aqueous solution. The maleimide group is more stable in aqueous solution than the NHS-ester group; therefore, conjugation experiments involving SMCC are usually performed with the amine targeted NHS-ester reaction being accomplished before sulfhydryl-targeted maleimide reaction in a two-step reaction procedure. According to this, conjugate **3** was synthesized through reaction of C6-amine modified 2-5A trimer pA3 with SMCC in phosphate buffer to form **2** followed by reaction with sulfhydryl containing compound **1** in good yield (Scheme 1). This method is the same as the one used for the preparation of previously reported ligand RBI1033.[34]

Preparation of phosphorothioated conjugate **5** was first tried using the same method as shown in Scheme 1. However, a side product was formed which didn't react with **1** in the second step reaction. It seems that the sulfhydryl group of spA was also involved in the reaction with SMCC. This side reaction was not reported when making **RBI1033** which also had phosphorothioate group in its structure. Attempts were made by conducting the reaction at pH 8.0 as reported for **RBI1033**, the same side product was observed. To avoid side reactions, the two-step conjugation was reversed by reaction of the maleimide group of SMCC with –SH group of **1** first followed by reaction of NHS-ester with amine group of 2-5A (Scheme 2). Because the NHS-ester undergoes hydrolytic degradation easily in the presence of water, the reaction must be carried out in anhydrous atmosphere. Hence, anhydrous DMF was used as the solvent instead of phosphate buffer. After reaction of SMCC with **1** in DMF at room temperature for 1 hour, C6-amine modified spA was added directly to the reaction mixture and new peaks were formed, which was confirmed by mass spectrometry to be conjugate **5**.

Conjugate **6** was prepared using the same method. By reversing the reaction steps and having the reaction carried out in anhydrous DMF instead of phosphate buffer, the new method was more efficient and time-saving.

To help investigate the importance of the 2-5A for the binding affinity, compounds **7** and **10** omitting 2-5A part were synthesized. Both compounds can be made using either method as shown in Scheme 2 or 3 and no purification is needed after first step coupling. Cleavage of the N-Boc group in **9** was achieved by addition of 4 M HCl in dioxane to get desired compound **10** (Scheme 3).

In order to get further evidence to support that the new ligands designed here are useful for imaging of prostate cancer, cold compounds **11** and **12** of future ^{18}F-radiolabelled analogues were synthesized. Terminal labeling of **5** and **6** was performed by reaction with N-(4-fluorobenzyl)-2-bromoacetamide (Scheme 2). This is a common method used to label oligonucleotide. Compared to **5** and **6**, compounds **11** and **12** have longer retention time due to increased lipophilicity following the addition of the halogenobenzyl substitution.

Compound **10** has a free amine in its structure, which makes it practical for labeling or derivatization. Compound **13** was made through amine reductive alkylation by the addition of 4-fluorobenzaldehyde together with sodium borohydride and fomic acid (Scheme 3). Another generally used method to label amine group is through reaction with excess amount of SFB, which was used to make compound **14**.

Competitive Binding Studies

All new compounds synthesized were evaluated in a competitive binding assay using tritium labeled S-methylated derivative of **1** (^{3}H-ZJ24) (Figure 1) as the radioligand to examine the ability of the novel compounds to compete for binding with ^{3}H-ZJ24 on LNCaP cells. Parent compound **1** was used as positive control. The results were listed in Table 1. Compounds **3**, **5** and **6** which contained 2-5A in their structures showed IC_{50} values at 1.6 nM, 0.11 nM and 0.012 nM respectively compared to parent compound **1** at 13.9 nM. Highest binding activity was found in compound **6** with spA3 in its structure.

In contrast, compounds **7** and **10** without 2-5A in structures showed dramatically decreased affinity to PSMA. Compound **7** gave an IC_{50} at 124 nM, which was about 9 fold higher than **1**; and compound **10** even had an IC_{50} as high as 363.1 nM. These results indicated that the integration of 2-5A plays a crucial role in PSMA binding, and that part can not be eliminated from structure.

After terminal labeling of 2-5A, the binding activity of compounds **11** (1.93 nM) and **12** (3.36 nM) was reduced compared to unlabeled compound **5** and **6**, however, still much better compared to parent ligand **1** (13.9 nM). Compounds **13** and **14** gave IC_{50} values at 95.3 nM and 169.9 nM respectively, which were improved, compared to the amine free compound **10** (361.3nM).

Inhibition of Folate Hydrose Activity

The new compounds were also evaluated by their ability to inhibit the folate hydrolase activity of PSMA to further confirm their affinity to PSMA. Methotrexate diglutamate was used as the substrate; the amount of methotrexate formed after incubation with PSMA positive LNCaP cell membrane was measured by HPLC. It was observed that the folate hydrolase activity of PSMA was significantly inhibited by the compounds containing 2-5A in their structure compared to the compounds omitting 2-5A. For example, at 10 nM concentration of inhibitors, the amount of MTX formed dropped below 20% for all the 2-5A conjugates (compounds **3**, **5, 6, 11** and **12)** compared to 45.3% for parent ligand **1**, while the amount of MTX formed was still higher than 75% for the compounds excluing 2-5A (compounds **7, 10, 13** and **14**) (Figure 2). The most two potent compounds were **5** and **6** with less than 30% MTX formed even at 1nM. Therefore, the inhibition of PSMA's folate hydroase activity of these compounds concurred with the competitive binding assay, which showed that incorporation of 2-5A in the structure rendered the compounds excellent bind affinity to PSMA.

Cytotoxicity of the conjugates

The cytotoxicity of the new compounds was test by incubating them with LNCaP cells. After incubation with LNCaP cells for 72 hours, none of the new conjugates showed any inhibition of LNCaP cell growth even at the concentration as high as 100 μM, which indicated that these conjugates are not toxic to LNCaP cells (Figure 3).

Discussion

In this paper, we reported the synthesis and biological activities of ten novel PSMA-based small compounds using the heterobifunctional linker SMCC to conjugate amine-containing molecules and the parent compound (S)-2-(3-((S)-5-amino-1-carboxypentyl)ureido)pentanedioic acid (**1**). Previously, we have reported that inclusion of a C3-amine modified 2-5A trimer into **1** through SMCC (RBI1033) improved its binding affinity 10 times.[34] Here we confirmed the observation again by preparation of a series of SMCC-ZJ24 analogues with or without 2-5A in their structures. It was observed that compounds with 2-5A in their structures showed significantly improved binding activity compared to those missing 2-5A. Extending the linker from C3 (RBI1033) to C6 (compound **6**) improved the binding activity more than 100 fold. It was also found that the binding affinity increased when the number of 2-5A increased from one (compound **5**) to three (compound **6**). Another interesting finding was that free 5'-phosphorothioate contributed to the activity greatly (compounds **5** and **6**), substitution of that group led to decreased activity (compounds **3**, **11** and **12**).

The crystal structure of PSMA has been well elucidated.[35-42] The active site contains two zinc atoms, a smaller pharmacophore binding site (S1') and a larger nonpharmacophore pocket (S1). According to these elucidated crystal structure of PSMA, the glutamate portion (P1') of our compounds should be undoubtly located in the S1' pocket of PSMA, while the remainder of the molecule (P1) should be oriented in the S1 pocket. The S1 pocket contains a ~20 Å deep tunnel which narrows gradually. Extension of C3 (RBI1033) to C6 (compound **6**) might have optimized the steric hindrance, thus leading to better fit and binding characteristic. The S1

pocket has an adjacent hydrophobic pocket and it is arginine-rich. It has been reported that introduction of phenyl group can improved the binding activity.[43, 44] Similar to phenyl group, adenine group from 2-5A can form hydrophobic binding with the pocket. On the other side, the negatively charged phosphorothioate groups of 2-5A can form strong ion pairs with the positively charged guarnidine groups of arginine. These two factors working together give the 2-5A containing compounds increased activity. Because the S1 pocket is positively charged, substitution of the free amine group in **10** neutralized its positive charge, hence gave improved binding activity as can be seen in compounds **13** and **14**. At this time, it's still not clear how the 5'-terminal phosphorothioate affect the binding. One hypothesis is that it might interact with the sulfhydryl group of cysteines in PSMA and form S-S bond.

As mentioned before, prostate cancer is the leading cancer in men and the second most common cause of cancer-related death. Furthermore, by the time of diagnosis only half of the tumors are clinically localized and half of these represent extracapsular spread.[45] Sensitive, functional imaging techniques are required to identify the extent of disease prior to therapy. PSMA provides an excellent target for prostate tumor imaging and therapy because of its transmembrane location and the fact that it is significantly upregulated in prostate cancer metastasis relative to the few normal tissues in which it resides at least hundred fold lower levels.[46] The phosphorothioated 2-5A containing compounds **5** and **6** can be easily labeled by coupling reaction of 5'-terminal phosphorothioate group with radiosynthon N-(4-[^{18}F]-fluorobenzyl)-2-bromoacetamide.[47] The corresponding cold compounds (**11** and **12**) showed excellent binding activities compared to parent compound **1**. Other groups have tried N-[N-(S)-1,3-dicarboxypropyl]-S-[^{11}C]methyl-L-cysteine ([^{11}C]-DCMC)[33], N-[N-(S)-1,3-dicarboxypropyl]carbamoyl]-4-[^{18}F]fluorobenzyl-L-cysteine ([^{18}F]-DCFBCA)[32] and ^{123}I-labled glutamtate-urea-lysine analogues ([^{123}I]MIP-702, [^{123}I]MIP-1095)[28]. They all showed selectively high uptake on PSMA-expressing tumor xenografts. Our compounds resemble part of the structures and have better binding affinity to PSMA. The future of using these ligands for imaging is very promising.

Conclusion

In summary, a series of novel urea-based PSMA ligand containing 4-(N-maleimidomethyl) cyclohexane-1-amidate linkage have been synthesized. Integration of 2-5A into the structure reveals outstanding activity in both competitive binding assay and inhibitory of folate hydroase activity assay. Compared to antibodies, these small molecules can be easily synthesized and are more cost effective. More importantly, they should have

favorable pharmacokinetic behaviors, such as fast uptake and quick clearance. The results reported in this paper provide supporting evidence for future 18-F radiolabeling as potential diagnostic imaging agents by targeting PSMA.

Experimental Section

Materials: Prostate cancer cell line LNCaP was obtained from American Type Culture Collection (ATCC). LNCaP cells were maintained in RPMI1640 medium supplemented with 2 mM L-glutamine and 10% Fetal Bovin Serum. N-[N-[(*S*)-1,3-dicarboxypropyl]carbamoyl]-L-cysteine (**1**) was custom made by Bachem Bioscience Inc. 3'-C6-amine modified oligonucleotides pApApA (pA3), spA and spAspAspA (spA3) were custom synthesized by GeneACT Inc, Japan. N-[N-[(*S*)-1,3-dicarboxypropyl]carbamoyl]-*S*-[^{3}H]-methyl-L-cysteine (^{3}H-ZJ24) was custom made by GE Healthcare Life Sciences. Succinimidyl 4-(N-maleimidomethyl)cyclohexane-1-carboxylate (SMCC) was purchased from Pierce. 4-amino-10-methylpteroyldi-γ-L-glutamic acid (MTXGlu2) was purchased from Schircks Laboratories, Switzerland. N-succimimidyl 4-fluorobenzoate (SFB) was ordered from ABX Advanced Biochemical Compounds, Germany. All the other chemicals were purchased from Sigma-Aldrich Inc., St. Louise, MO, USA. High resolution mass spectra were obtained from an Applied Biosystems 4800 MALDI TOF/TOF Analyzer using positive ion electrospray.

Synthesis of pA3-SMCC (**2**). To a solution of pA3-C6-NH2 (900 μg, 0.8 μmol) in 100 uL of 100 mM phosphate buffer (pH 7.0) was added 14 mg of sulfo-SMCC (32 μmol) in 1mL of 100 mM phosphate buffer (pH 7.0). After stirring at room temperature (r.t.) overnight, the mixture was purified by preparative HPLC to obtain the desired product at 72.8% yield (815 μg). Retention time (Rt) = 23.5min. MALDI MS m/z: 1404 (M+1).

Synthesis of pA3-SMCC-ZJ24 (**3**). To a solution of **2** (300 μg, 0.2 μmol) in 400 μL of 100 mM phosphate buffer (pH 7.0) was added 500 μg of **1** (1.0 μmol). After stirring at r.t. for 1 hour, the mixture was purified by preparative HPLC to get the final product at 89.8% yield (300 μg). Rt = 17.5 min. MALDI MS m/z: 1698 (M+1).

Synthesis of spA-SMCC-ZJ24 (**5**). SMCC 10mg (0.03 mmol) was dissolved in 500uL N,N-dimethylformide (DMF), then 17mg of **1** (0.06 mmol) in 500uL DMF was added. After stirring at r.t. for 1 hr, 0.2 mg of spA (0.0035 mmol) was added. The mixture was stirred at r.t. overnight, then applied to preparative HPLC to give the purified product at 90% yield (0.35 mg). Rt = 13.4 min. MALDI MS m/z: 1072 (M+1).

Synthesis of spA3-SMCC-ZJ24 (**6**). The compound was synthesized using the same method as spA-SMCC-ZJ24. Rt = 13.9 min. MALDI MS m/z: 1762 (M+1).

Synthesis of 4-F-SMCC-ZJ24 (**7**). The compound was synthesized using the same method as **5**. Rt = 22.3 min. MALDI MS m/z: 639 (M+1).

Synthesis of Boc-C6-SMCC-ZJ24 (**9**). SMCC 1 mg (0.003 mmol) was dissolved in 1 mL anhydrous acetonitrile, then N-Boc-1, 6-diaminohexane (1.3 μL, 0.006 mmol) was added. After stirring at r.t. for 2 hr, 1.7 mg of **1** (0.006 mmol) in 0.5 mL 100 mM phosphate was added. The mixture was stirred for another hour, then applied to preparative HPLC to get purified product with a yield of 84% (1.8 mg). Rt = 22.1 min. MALDI MS m/z: 768 (M+K).

Synthesis of $NH3^+$-C6-SMCC-ZJ24 (**10**). Boc-C6-SMCC-ZJ24 (1 mg, 0.0014 mmol) was dissolved in 1 mL of 6 M HCl/dioxane. After stirring at r.t. for 1 hr, the solvent was removed to give the dry product with a yield of 97% (0.9 mg). Rt = 13.5 min. MALDI MS m/z: 666 (M+1).

Synthesis of N-(4-fluorobenzyl)-2-bromoacetamide.[47] To a solution containing 4-fluorobenzylamine (1.25 g, 10mmol) and N-methylmorhpoline (1.0 g, 10mmol) in 25 mL of dichloromethane was added bromoacetyl bromide (2.0 g, 20 mmol). After addition, the reaction mixture was stirred at r.t. overnight. The mixture was then filtered and concentrated to dryness, and the residual was purified on a silica column. Elution with hexane/ ethyl acetate (9:1) gave the pure product as light yellow solid (2.1 g, 87.5%). ^{1}H NMR ($CDCl_3$) δ 7.25 (d, 2H), 7.04 (d, 2H), 4.45 (d, 2H), 3.93 (s, 2H).

Synthesis of 4-F-spA-SMCC-ZJ24 (**11**).[47] To a solution of **5** (200 μg, 0.19 μmol) in 1 mL of methanol-phosphate buffer (100mM, pH 8.0) was added excess amount of N-(4-fluorobenzyl)-2-bromoacetamide (240 μg, 0.95 μmol). The mixture was stirred at 120^{o}C for 30 min, then the solvent was evaporated and the products was purified by preparative HPLC (214 μg, 91.3%). Rt = 27.5 min. MALDI MS m/z: 1237 (M+1).

Synthesis of 4-F-spA3-SMCC-ZJ24 (**12**). The compound was synthesized using the same method as 4-F-spA-SMCC-ZJ24. Rt = 11.6 min. MALDI MS m/z: 1927 (M+1).

Synthesis of 4-F-benzyl-C6-SMCC-ZJ24 (**13**). To a solution of **10** (1 mg, 0.0015 mmol) in 1 mL of anhydrous methanol was added 4-fluorobenzaldehyde (0.3 μL, 0.003 mmol), $NaBH_3CN$ (0.2 mg, 0.003 mmol) and acetic acid (1 μL). The reaction mixture was stirred at room temperature for 2 hrs; then separated by preparative HPLC to give the final product in a yield of 72% (0.8 mg). Rt = 19.3 min. MALDI MS m/z: 738 (M+1).

Synthesis of 4-F-phenyl-C6-SMCC-ZJ24 (**14**).[48] To a solution of **10** (3.8 mg, 0.006 mmol) in 1 mL of anhydrous methanol was added triethylamine (5 μL), followed by SFB (3 mg, 0.012 mmol). After stirring at room temperature for 2 hrs, the solvent was removed and the product was separated by preparative HPLC with a yield of 85% (3.8 mg). Rt = 23.4 min. MALDI MS m/z: 752 (M+1).

High performance liquid chromatography (HPLC). HPLC was performed using a Shimadzu HPLC system equipped with a SPD-20V prominence UV/visible detector and monitored at a wavelength at 260 nm. The gradient used is 0-55% B over 45 minutes (A is 10 mM triethylammonium acetate TEAA, pH 7.0; B is acetonitrile). Analytical HPLC was performed using an analytical Symmetry C18 column (150 mm × 4.6 mm × 5μm, Waters Corporation, Milford, MA, USA)) at a flow rate of 1 mL/min. Preparative HPLC was achieved using SymmetryPrep^{TM} C18 column (100mm × 19 mm × 5μm) at a flow rate of 3.0 ml/min.

Competitive binding assay. Briefly, LNCaP cells (5×10^5) were incubated with different concentrations of ligands in the presence of 12 nM ^{3}H-ZJ24 in a total volume of 300 μL for 1 hour at 37^{o}C. The mixture was centrifuged at 1,000 g for 5 min at 4^{o}C, then washed three time with 500 μL of cold PBS. Finally, 4 mL of EcoLume^{TM} cocktail (MP Biomedicals) was added, and radioactivity was counted by scintillation counter. The concentration required to inhibit 50% of binding is determined (IC_{50}) by GraphPad Prism 3.0.

Folate hydrolase inhibitory assay. LNCaP cell membrane (10 μg) was incubated with ligands in the presence of 5 nMol of the polyglutamate substrate methotrexate diglutamate ($MTXGlu_2$) for 1 hr at 37 °C. The reaction was stopped by the addition of 100 μL of 50 mM Na_2HPO_4. The amount of methotrexate (MTX) formed was analyzed using a Thermo Hypersil PRISM RP column (50 x 4.6 mm, flow rate 1.0mL/min) at 313 nm using a mobile phase of 50mM phosphate buffer/methanol (85/50).

In vitro cytotoxicity assay. Cytotoxicity of the new conjugate against PSMA positive LNCaP cells was test using the colorimetric CellTiter 96 Aqueous Cell Proliferation Assay (Promega). Briefly, cells were seeded in 96-well culture plates at a density of 3,000 cells/well the day before treatment. Drugs were added after serial dilution and exposed to the cells for 72 hours. CellTiter 96 Aqueous reagent was then added to each well. After a 3-hour incubation period at 37 °C, the absorbance at 490 nm was measured with a 96-well plate reader and the IC_{50} values were determined.

Acknowledgement

This work was supported by a grant from Department of Defense (DOD) (Grant W81XWH-07-1-0656).

References:

1. Jemal, A.; Siegel, R.; Ward, E.; Hao, Y.; Xu, J.; Thun, M. J., Cancer statistics, 2009. *CA Cancer J Clin* **2009,** 59, (4), 225-49.

2. Horoszewicz, J. S.; Kawinski, E.; Murphy, G. P., Monoclonal antibodies to a new antigenic marker in epithelial prostatic cells and serum of prostatic cancer patients. *Anticancer Res.* **1987,** 7, (5B), 927-35.

3. Israeli, R. S.; Powell, C. T.; Corr, J. G.; Fair, W. R.; Heston, W. D., Expression of the prostate-specific membrane antigen. *Cancer Res.* **1994,** 54, (7), 1807-11.

4. Tasch, J.; Gong, M.; Sadelain, M.; Heston, W. D., A unique folate hydrolase, prostate-specific membrane antigen (PSMA): a target for immunotherapy? *Crit. Rev. Immunol.* **2001,** 21, (1-3), 249-61.

5. Wright, G. L., Jr.; Grob, B. M.; Haley, C.; Grossman, K.; Newhall, K.; Petrylak, D.; Troyer, J.; Konchuba, A.; Schellhammer, P. F.; Moriarty, R., Upregulation of prostate-specific membrane antigen after androgen-deprivation therapy. *Urology* **1996,** 48, (2), 326-34.

6. Bostwick, D. G.; Pacelli, A.; Blute, M.; Roche, P.; Murphy, G. P., Prostate specific membrane antigen expression in prostatic intraepithelial neoplasia and adenocarcinoma: a study of 184 cases. *Cancer* **1998,** 82, (11), 2256-61.

7. Troyer, J. K.; Beckett, M. L.; Wright, G. L., Jr., Detection and characterization of the prostate-specific membrane antigen (PSMA) in tissue extracts and body fluids. *Int. J. Cancer* **1995,** 62, (5), 552-8.

8. Chang, S. S.; Reuter, V. E.; Heston, W. D.; Bander, N. H.; Grauer, L. S.; Gaudin, P. B., Five different anti-prostate-specific membrane antigen (PSMA) antibodies confirm PSMA expression in tumor-associated neovasculature. *Cancer Res.* **1999,** 59, (13), 3192-8.

9. Kahn, D.; Williams, R. D.; Seldin, D. W.; Libertino, J. A.; Hirschhorn, M.; Dreicer, R.; Weiner, G. J.; Bushnell, D.; Gulfo, J., Radioimmunoscintigraphy with 111indium labeled CYT-356 for the detection of occult prostate cancer recurrence. *J. Urol.* **1994,** 152, (5 Pt 1), 1490-5.

10. Liu, H.; Moy, P.; Kim, S.; Xia, Y.; Rajasekaran, A.; Navarro, V.; Knudsen, B.; Bander, N. H., Monoclonal antibodies to the extracellular domain of prostate-specific membrane antigen also react with tumor vascular endothelium. *Cancer Res.* **1997,** 57, (17), 3629-34.

11. Gregorakis, A. K.; Holmes, E. H.; Murphy, G. P., Prostate-specific membrane antigen: current and future utility. *Semin. Urol. Oncol.* **1998,** 16, (1), 2-12.

12. Smith-Jones, P. M.; Vallabhajosula, S.; Navarro, V.; Bastidas, D.; Goldsmith, S. J.; Bander, N. H., Radiolabeled monoclonal antibodies specific to the extracellular domain of prostate-specific membrane antigen: preclinical studies in nude mice bearing LNCaP human prostate tumor. *J. Nucl. Med.* **2003,** 44, (4), 610-7.

13. Holmes, E. H., PSMA specific antibodies and their diagnostic and therapeutic use. *Expert Opin. Investig. Drugs* **2001,** 10, (3), 511-9.

14. McDevitt, M. R.; Barendswaard, E.; Ma, D.; Lai, L.; Curcio, M. J.; Sgouros, G.; Ballangrud, A. M.; Yang, W. H.; Finn, R. D.; Pellegrini, V.; Geerlings, M. W., Jr.; Lee, M.; Brechbiel, M. W.; Bander, N. H.; Cordon-Cardo, C.; Scheinberg, D. A., An alpha-particle emitting antibody ([213Bi]J591) for radioimmunotherapy of prostate cancer. *Cancer Res* **2000,** 60, (21), 6095-100.

15. Bander, N. H.; Nanus, D. M.; Milowsky, M. I.; Kostakoglu, L.; Vallabahajosula, S.; Goldsmith, S. J., Targeted systemic therapy of prostate cancer with a monoclonal antibody to prostate-specific membrane antigen. *Semin. Oncol.* **2003,** 30, (5), 667-76.

16. Nanus, D. M.; Milowsky, M. I.; Kostakoglu, L.; Smith-Jones, P. M.; Vallabahajosula, S.; Goldsmith, S. J.; Bander, N. H., Clinical use of monoclonal antibody HuJ591 therapy: targeting prostate specific membrane antigen. *J. Urol.* **2003,** 170, (6 Pt 2), S84-8; discussion S88-9.

17. Bander, N. H.; Trabulsi, E. J.; Kostakoglu, L.; Yao, D.; Vallabhajosula, S.; Smith-Jones, P.; Joyce, M. A.; Milowsky, M.; Nanus, D. M.; Goldsmith, S. J., Targeting metastatic prostate cancer with radiolabeled monoclonal antibody J591 to the extracellular domain of prostate specific membrane antigen. *J. Urol.* **2003,** 170, (5), 1717-21.

18. Milowsky, M. I.; Nanus, D. M.; Kostakoglu, L.; Sheehan, C. E.; Vallabhajosula, S.; Goldsmith, S. J.; Ross, J. S.; Bander, N. H., Vascular targeted therapy with anti-prostate-specific membrane antigen monoclonal antibody J591 in advanced solid tumors. *J Clin Oncol* **2007,** 25, (5), 540-7.

19. Galsky, M. D.; Eisenberger, M.; Moore-Cooper, S.; Kelly, W. K.; Slovin, S. F.; DeLaCruz, A.; Lee, Y.; Webb, I. J.; Scher, H. I., Phase I trial of the prostate-specific membrane antigen-directed immunoconjugate MLN2704 in patients with progressive metastatic castration-resistant prostate cancer. *J Clin Oncol* **2008,** 26, (13), 2147-54.

20. Carter, R. E.; Feldman, A. R.; Coyle, J. T., Prostate-specific membrane antigen is a hydrolase with substrate and pharmacologic characteristics of a neuropeptidase. *Proc Natl Acad Sci U S A* **1996,** 93, (2), 749-53.

21. Pinto, J. T.; Suffoletto, B. P.; Berzin, T. M.; Qiao, C. H.; Lin, S.; Tong, W. P.; May, F.; Mukherjee, B.; Heston, W. D., Prostate-specific membrane antigen: a novel folate hydrolase in human prostatic carcinoma cells. *Clin. Cancer Res.* **1996,** 2, (9), 1445-51.

22. Slusher, B. S.; Vornov, J. J.; Thomas, A. G.; Hurn, P. D.; Harukuni, I.; Bhardwaj, A.; Traystman, R. J.; Robinson, M. B.; Britton, P.; Lu, X. C.; Tortella, F. C.; Wozniak, K. M.; Yudkoff, M.; Potter, B. M.; Jackson, P. F., Selective inhibition of NAALADase, which converts NAAG to glutamate, reduces ischemic brain injury. *Nat. Med.* **1999,** 5, (12), 1396-402.

23. Kozikowski, A. P.; Nan, F.; Conti, P.; Zhang, J.; Ramadan, E.; Bzdega, T.; Wroblewska, B.; Neale, J. H.; Pshenichkin, S.; Wroblewski, J. T., Design of remarkably simple, yet potent urea-based inhibitors of glutamate carboxypeptidase II (NAALADase). *J. Med. Chem.* **2001,** 44, (3), 298-301.

24. Jackson, P. F.; Tays, K. L.; Maclin, K. M.; Ko, Y. S.; Li, W.; Vitharana, D.; Tsukamoto, T.; Stoermer, D.; Lu, X. C.; Wozniak, K.; Slusher, B. S., Design and pharmacological activity of phosphinic acid based NAALADase inhibitors. *J. Med. Chem.* **2001,** 44, (24), 4170-5.

25. Tang, H.; Brown, M.; Ye, Y.; Huang, G.; Zhang, Y.; Wang, Y.; Zhai, H.; Chen, X.; Shen, T. Y.; Tenniswood, M., Prostate targeting ligands based on N-acetylated alpha-linked acidic dipeptidase. *Biochem. Biophys. Res. Commun.* **2003,** 307, (1), 8-14.

26. Majer, P.; Jackson, P. F.; Delahanty, G.; Grella, B. S.; Ko, Y. S.; Li, W.; Liu, Q.; Maclin, K. M.; Polakova, J.; Shaffer, K. A.; Stoermer, D.; Vitharana, D.; Wang, E. Y.; Zakrzewski, A.; Rojas, C.; Slusher, B. S.; Wozniak, K. M.; Burak, E.; Limsakun, T.; Tsukamoto, T., Synthesis and biological evaluation of thiol-based inhibitors of glutamate carboxypeptidase II: discovery of an orally active GCP II inhibitor. *J. Med. Chem.* **2003,** 46, (10), 1989-96.

27. Kozikowski, A. P.; Nan, F.; Conti, P.; Zhang, J.; Ramadan, E.; Bzdega, T.; Wroblewska, B.; Neale, J. H.; Pshenichkin, S.; Wroblewski, J. T., Design of remarkably simple, yet potent urea-based inhibitors of glutamate carboxypeptidase II (NAALADase). *J Med Chem* **2001,** 44, (3), 298-301.

28. Hillier, S. M.; Maresca, K. P.; Femia, F. J.; Marquis, J. C.; Foss, C. A.; Nguyen, N.; Zimmerman, C. N.; Barrett, J. A.; Eckelman, W. C.; Pomper, M. G.; Joyal, J. L.; Babich, J. W., Preclinical evaluation of novel glutamate-urea-lysine analogues that target prostate-specific membrane antigen as molecular imaging pharmaceuticals for prostate cancer. *Cancer Res* **2009,** 69, (17), 6932-40.

29. Chen, Y.; Foss, C. A.; Byun, Y.; Nimmagadda, S.; Pullambhatla, M.; Fox, J. J.; Castanares, M.; Lupold, S. E.; Babich, J. W.; Mease, R. C.; Pomper, M. G., Radiohalogenated prostate-specific membrane antigen (PSMA)-based ureas as imaging agents for prostate cancer. *J Med Chem* **2008,** 51, (24), 7933-43.

30. Chandran, S. S.; Banerjee, S. R.; Mease, R. C.; Pomper, M. G.; Denmeade, S. R., Characterization of a targeted nanoparticle functionalized with a urea-based inhibitor of prostate-specific membrane antigen (PSMA). *Cancer Biol Ther* **2008,** 7, (6), 974-82.

31. Banerjee, S. R.; Foss, C. A.; Castanares, M.; Mease, R. C.; Byun, Y.; Fox, J. J.; Hilton, J.; Lupold, S. E.; Kozikowski, A. P.; Pomper, M. G., Synthesis and evaluation of technetium-99m- and rhenium-labeled inhibitors of the prostate-specific membrane antigen (PSMA). *J Med Chem* **2008,** 51, (15), 4504-17.

32. Mease, R. C.; Dusich, C. L.; Foss, C. A.; Ravert, H. T.; Dannals, R. F.; Seidel, J.; Prideaux, A.; Fox, J. J.; Sgouros, G.; Kozikowski, A. P.; Pomper, M. G., N-[N-[(S)-1,3-Dicarboxypropyl]carbamoyl]-4-[18F]fluorobenzyl-L-cysteine, [18F]DCFBC: a new imaging probe for prostate cancer. *Clin Cancer Res* **2008,** 14, (10), 3036-43.

33. Foss, C. A.; Mease, R. C.; Fan, H.; Wang, Y.; Ravert, H. T.; Dannals, R. F.; Olszewski, R. T.; Heston, W. D.; Kozikowski, A. P.; Pomper, M. G., Radiolabeled small-molecule ligands for prostate-specific membrane antigen: in vivo imaging in experimental models of prostate cancer. *Clin Cancer Res* **2005,** 11, (11), 4022-8.

34. Cramer, H.; Okicki, J. R.; Rho, T.; Wang, X.; Silverman, R. H.; Heston, W. D., 2-5A ligands--a new concept for the treatment of prostate cancer. *Nucleosides Nucleotides Nucleic Acids* **2007,** 26, (10-12), 1471-7.

35. Davis, M. I.; Bennett, M. J.; Thomas, L. M.; Bjorkman, P. J., Crystal structure of prostate-specific membrane antigen, a tumor marker and peptidase. *Proc Natl Acad Sci U S A* **2005,** 102, (17), 5981-6.

36. Mesters, J. R.; Henning, K.; Hilgenfeld, R., Human glutamate carboxypeptidase II inhibition: structures of GCPII in complex with two potent inhibitors, quisqualate and 2-PMPA. *Acta Crystallogr D Biol Crystallogr* **2007,** 63, (Pt 4), 508-13.

37. Hlouchova, K.; Barinka, C.; Konvalinka, J.; Lubkowski, J., Structural insight into the evolutionary and pharmacologic homology of glutamate carboxypeptidases II and III. *Febs J* **2009,** 276, (16), 4448-62.

38. Barinka, C.; Byun, Y.; Dusich, C. L.; Banerjee, S. R.; Chen, Y.; Castanares, M.; Kozikowski, A. P.; Mease, R. C.; Pomper, M. G.; Lubkowski, J., Interactions between human glutamate carboxypeptidase II and urea-based inhibitors: structural characterization. *J Med Chem* **2008,** 51, (24), 7737-43.

39. Barinka, C.; Hlouchova, K.; Rovenska, M.; Majer, P.; Dauter, M.; Hin, N.; Ko, Y. S.; Tsukamoto, T.; Slusher, B. S.; Konvalinka, J.; Lubkowski, J., Structural basis of interactions between human glutamate carboxypeptidase II and its substrate analogs. *J Mol Biol* **2008,** 376, (5), 1438-50.

40. Barinka, C.; Rovenska, M.; Mlcochova, P.; Hlouchova, K.; Plechanovova, A.; Majer, P.; Tsukamoto, T.; Slusher, B. S.; Konvalinka, J.; Lubkowski, J., Structural insight into the pharmacophore pocket of human glutamate carboxypeptidase II. *J Med Chem* **2007,** 50, (14), 3267-73.

41. Barinka, C.; Starkova, J.; Konvalinka, J.; Lubkowski, J., A high-resolution structure of ligand-free human glutamate carboxypeptidase II. *Acta Crystallogr Sect F Struct Biol Cryst Commun* **2007,** 63, (Pt 3), 150-3.

42. Mesters, J. R.; Barinka, C.; Li, W.; Tsukamoto, T.; Majer, P.; Slusher, B. S.; Konvalinka, J.; Hilgenfeld, R., Structure of glutamate carboxypeptidase II, a drug target in neuronal damage and prostate cancer. *Embo J* **2006,** 25, (6), 1375-84.

43. Maung, J.; Mallari, J. P.; Girtsman, T. A.; Wu, L. Y.; Rowley, J. A.; Santiago, N. M.; Brunelle, A. N.; Berkman, C. E., Probing for a hydrophobic a binding register in prostate-specific membrane antigen with phenylalkylphosphonamidates. *Bioorg Med Chem* **2004,** 12, (18), 4969-79.

44. Kularatne, S. A.; Wang, K.; Santhapuram, H. K.; Low, P. S., Prostate-specific membrane antigen targeted imaging and therapy of prostate cancer using a PSMA inhibitor as a homing ligand. *Mol Pharm* **2009,** 6, (3), 780-9.

45. Kotzerke, J.; Gschwend, J. E.; Neumaier, B., PET for prostate cancer imaging: still a quandary or the ultimate solution? *J. Nucl. Med.* **2002,** 43, (2), 200-2.

46. O'Keefe, D. S.; Bacich, D. J.; Heston, W. D., Comparative analysis of prostate-specific membrane antigen (PSMA) versus a prostate-specific membrane antigen-like gene. *Prostate* **2004,** 58, (2), 200-10.

47. Kuhnast, B.; Dolle, F.; Terrazzino, S.; Rousseau, B.; Loc'h, C.; Vaufrey, F.; Hinnen, F.; Doignon, I.; Pillon, F.; David, C.; Crouzel, C.; Tavitian, B., General method to label antisense oligonucleotides with radioactive halogens for pharmacological and imaging studies. *Bioconjug Chem* **2000,** 11, (5), 627-36.

48. Vaidyanathan, G.; Zalutsky, M. R., Improved synthesis of N-succinimidyl 4-[18F]fluorobenzoate and its application to the labeling of a monoclonal antibody fragment. *Bioconjug Chem* **1994,** 5, (4), 352-6.

Table 1. Competitive binding activity of new compounds

Compounds	IC_{50} (nM)
Cys-CO-Glu **(1)**	13.9
RBI1033	1.5[34]
pA3-SMCC-ZJ24 **(3)**	1.6
spA-SMCC-ZJ24 **(5)**	0.11
spA3-SMCC-ZJ24 **(6)**	0.012
4-F-SMCC-ZJ24 **(7)**	124.0
NH_2-SMCC-ZJ24 **(10)**	363.1
4-F-spA-SMCC-ZJ24 **(11)**	1.93
4-F-spA-SMCC-ZJ24 **(12)**	3.36
4-F-benzyl-C6-SMCC-ZJ24 (**13)**	95.4
4-F-phenzyl-C6-SMCC-ZJ24 (**14)**	169.9

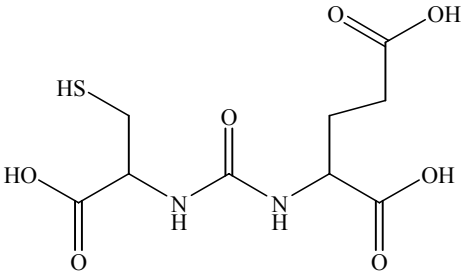

Cys-(CO)-Glu (1)

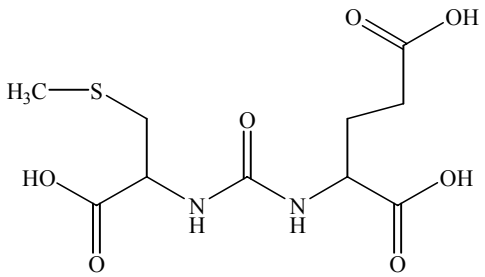

ZJ24

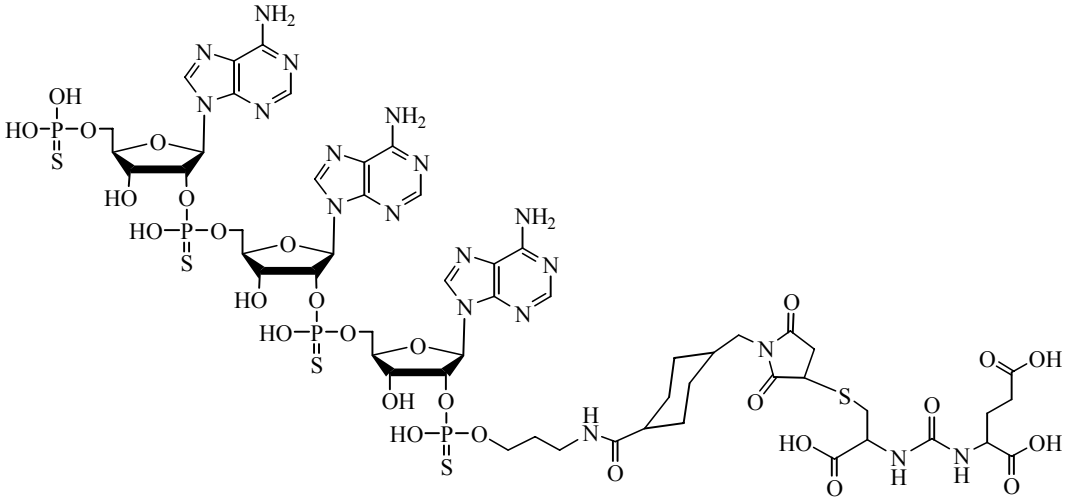

RBI 1033

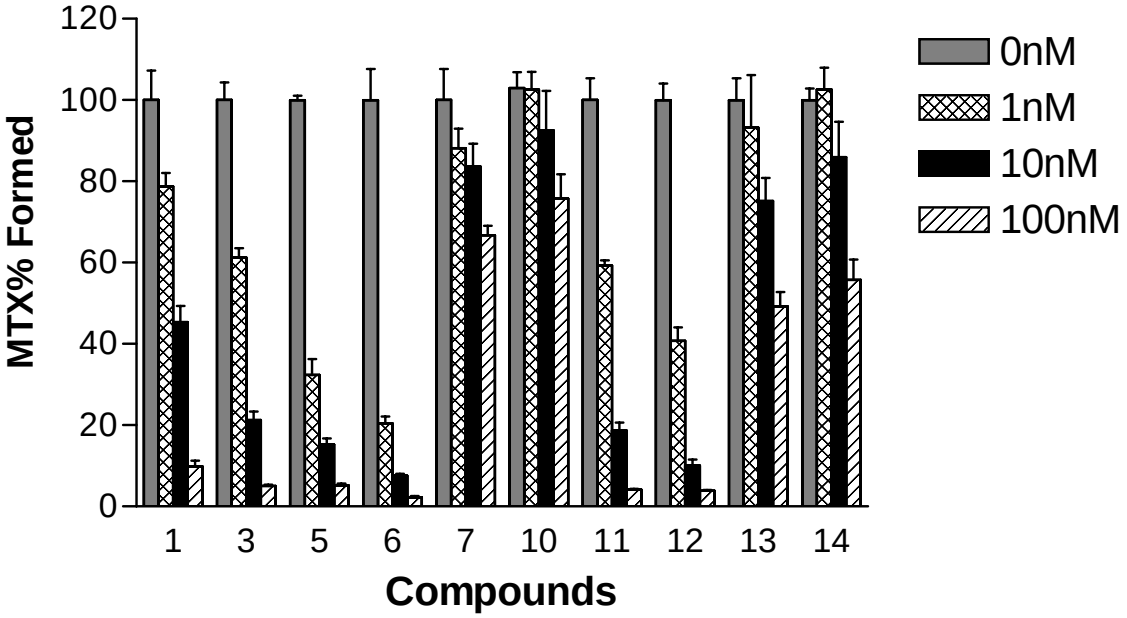
120
100
80
60
40
20
0
MTX% Formed
1
3
5
6
7
10
11
12
13
14
Compounds
0nM
1nM
10nM
100nM

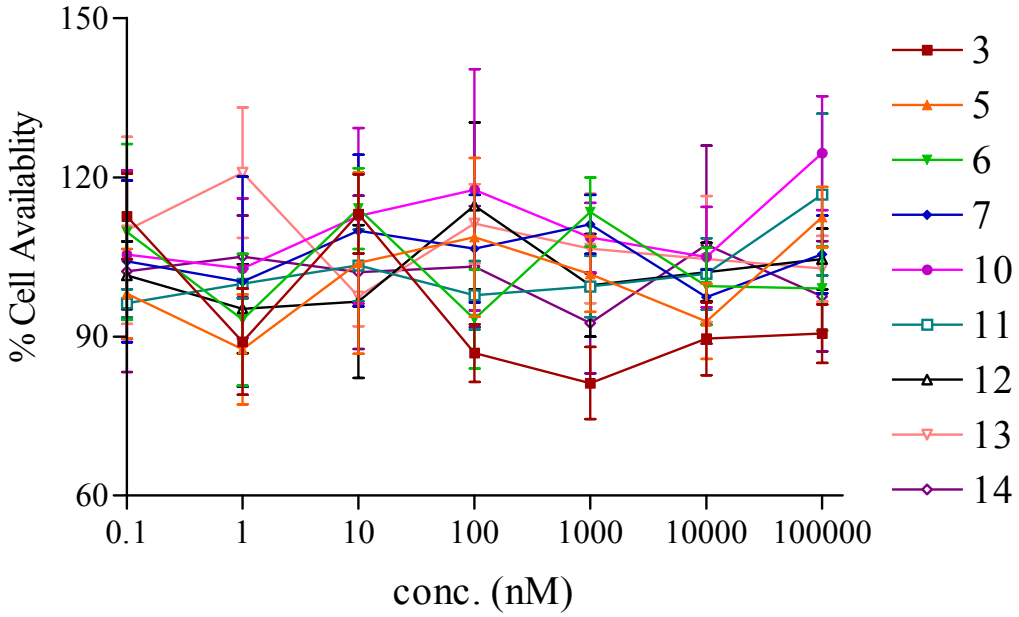
150
120
90
60
% Cell Availablity
0.1
1
10
100
1000
10000
100000
conc. (nM)
3
5
6
7
10
11
12
13
14

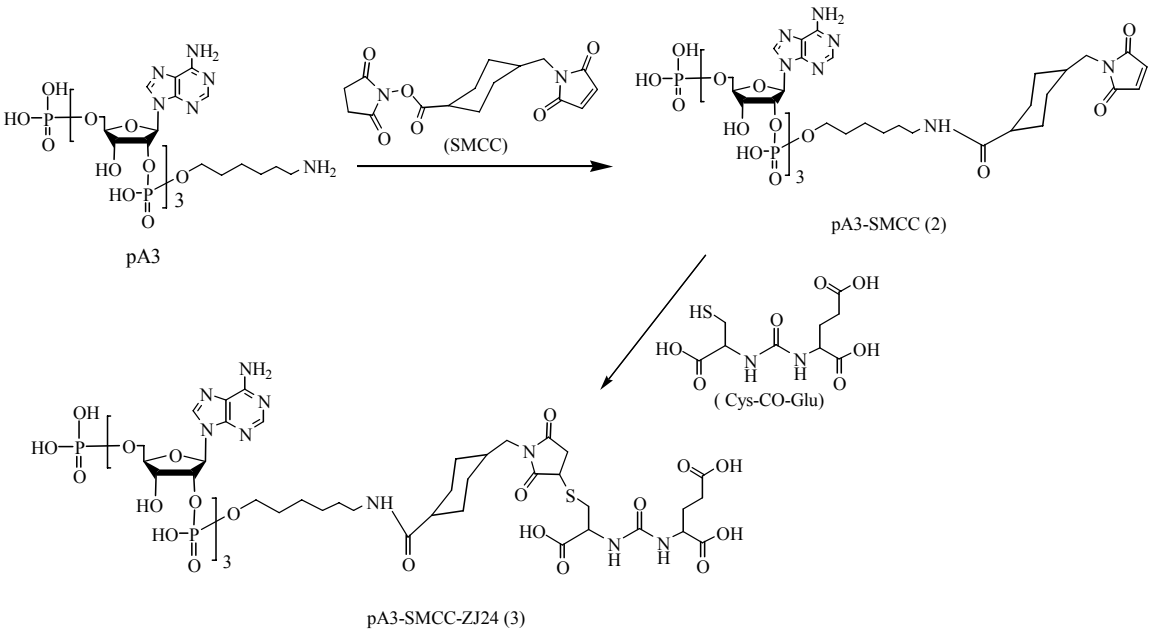
(SMCC)
pA3
pA3-SMCC (2)
(Cys-CO-Glu)
pA3-SMCC-ZJ24 (3)

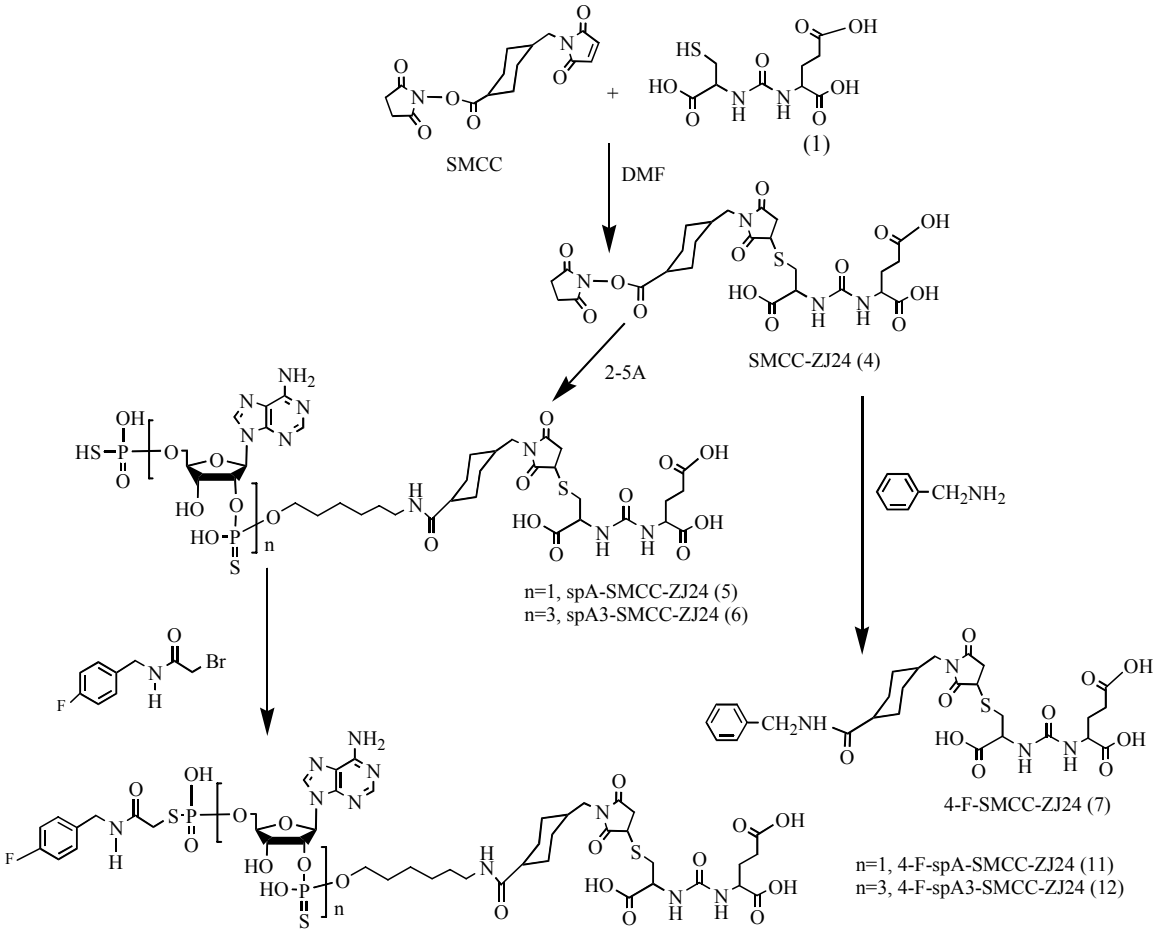
SMCC
(1)
DMF
SMCC-ZJ24 (4)
2-5A
n=1, spA-SMCC-ZJ24 (5)
n=3, spA3-SMCC-ZJ24 (6)
4-F-SMCC-ZJ24 (7)
n=1, 4-F-spA-SMCC-ZJ24 (11)
n=3, 4-F-spA3-SMCC-ZJ24 (12)

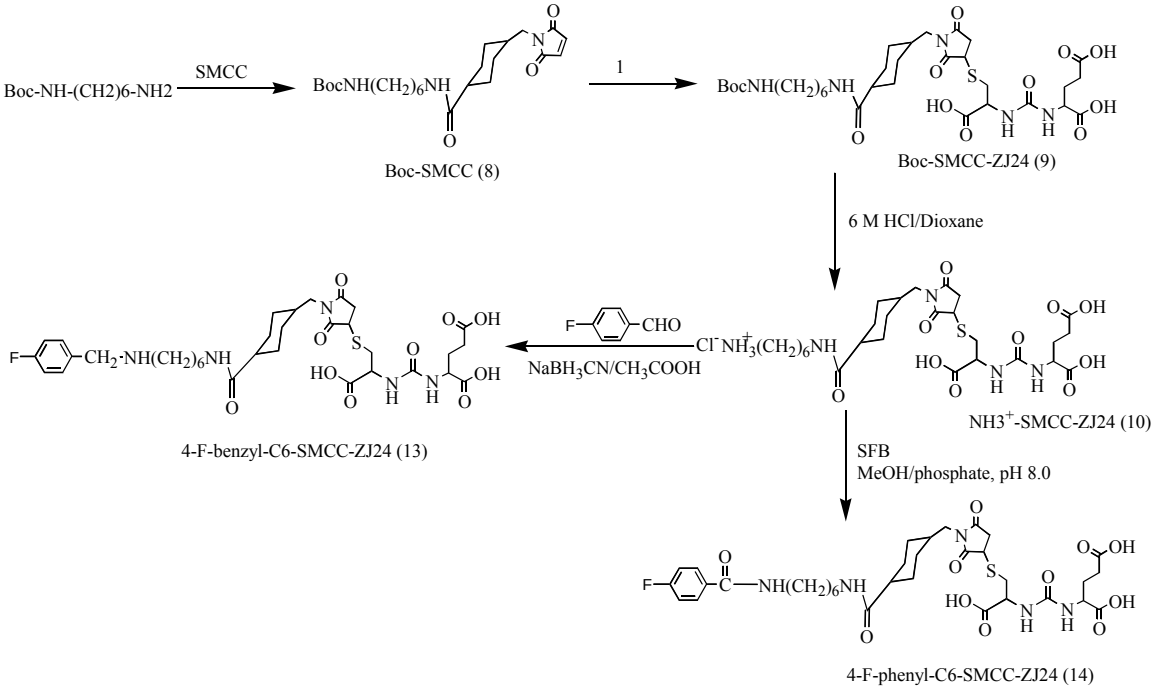
Boc-NH-(CH2)6-NH2
SMCC
BocNH(CH2)6NH
Boc-SMCC (8)
1
Boc-SMCC-ZJ24 (9)
6 M HCl/Dioxane
NH3+-SMCC-ZJ24 (10)
F-CHO
NaBH3CN/CH3COOH
4-F-benzyl-C6-SMCC-ZJ24 (13)
SFB
MeOH/phosphate, pH 8.0
4-F-phenyl-C6-SMCC-ZJ24 (14)

Table of Contents Graphic